

UNCLASSIFIED

AD NUMBER

ADB024910

LIMITATION CHANGES

TO:

Approved for public release; distribution is unlimited.

FROM:

Distribution authorized to U.S. Gov't. agencies only; Test and Evaluation; OCT 1977. Other requests shall be referred to Air Force Flight Dynamics Lab., Wright-Patterson AFB, OH 45433.

AUTHORITY

AFWAL ltr 10 Jun 1982

THIS PAGE IS UNCLASSIFIED

AD

B024910

AUTHORITY:

REFUGAL

10340 82



✓

AFFDL-TR-77-111

②

H

AD B024910

**MINIMUM WEIGHT DESIGN OF CYLINDRICAL SHELL
WITH MULTIPLE STIFFENER SIZES UNDER BUCKLING
CONSTRAINT**

*SCHOOL OF AERONAUTICS AND ASTRONAUTICS
PURDUE UNIVERSITY
WEST LAFAYETTE, INDIANA 47907*

OR

291850

DDC
FEB 15 1978
F

NO. _____
DUC FILE COPY

OCTOBER 1977

TECHNICAL REPORT AFFDL-TR-77-111
Final Report for Period June 1976 - October 1977

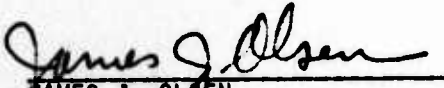
Distribution limited to U.S. Government agencies only; test and evaluation; statement applied in October 1977. Other requests for this document must be referred to Air Force Flight Dynamics Laboratory (FBR), Wright-Patterson Air Force Base, Ohio 45433.


AIR FORCE FLIGHT DYNAMICS LABORATORY
AIR FORCE WRIGHT AERONAUTICAL LABORATORIES
AIR FORCE SYSTEMS COMMAND
WRIGHT-PATTERSON AIR FORCE BASE, OHIO 45433

NOTICE

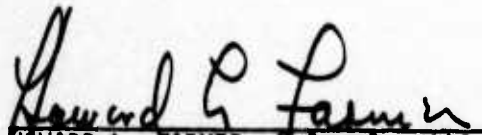
When Government drawings, specifications, or other data are used for any purpose other than in connection with a definitely related Government procurement operation, the United States Government thereby incurs no responsibility nor any obligation whatsoever; and the fact that the Government may have formulated, furnished, or in any way supplied the said drawings, specifications, or other data, is not to be regarded by implication or otherwise as in any manner licensing the holder or any other person or corporation, or conveying any rights or permission to manufacture, use, or sell any patented invention that may in any way be related thereto.

This technical report has been reviewed and is approved for publication.


JAMES J. OLSEN
Project Engineer


RICHARD D. KROBUSEK, Major, USAF
Ch, Analysis & Optimization Br

FOR THE COMMANDER


HOWARD L. FARMER, Colonel, USAF
Chief, Structural Mechanics Division

Copies of this report should not be returned unless return is required by security considerations, contractual obligations, or notice on a specific document.

UNCLASSIFIED

SECURITY CLASSIFICATION OF THIS PAGE (When Data Entered)

19 REPORT DOCUMENTATION PAGE		READ INSTRUCTIONS BEFORE COMPLETING FORM	
1. REPORT NUMBER 18 AFFDL-TR-77-111 ✓	2. GOVT ACCESSION NO.	3. RECIPIENT'S CATALOG NUMBER	
6 4. TITLE (and Subtitle) MINIMUM WEIGHT DESIGN OF CYLINDRICAL SHELL WITH MULTIPLE STIFFENER SIZES UNDER BUCKLING CONSTRAINT.		9 5. TYPE OF REPORT & PERIOD COVERED Final Report Jun 1976 - Oct 1977	
		6. PERFORMING ORG. REPORT NUMBER	
10 7. AUTHOR(s) T. Y. YANG	15 8. CONTRACT OR GRANT NUMBER(s) F33615-76-C-3145		
9. PERFORMING ORGANIZATION NAME AND ADDRESS School of Aeronautics and Astronautics Purdue University West Lafayette, Indiana 47907 ✓		10. PROGRAM ELEMENT, PROJECT, TASK AREA & WORK UNIT NUMBERS PE61102F, 17 05 WD23070501 16	
11. CONTROLLING OFFICE NAME AND ADDRESS AFSC (AFWAL) AF Flight Dynamics Laboratory (FBR) Structural Mechanics Division, WPAFB, OHIO 45433		11. REPORT DATE Oct 1977 12 173A	
14. MONITORING AGENCY NAME & ADDRESS (if different from Controlling Office)		12. NUMBER OF PAGES 61	
		15. SECURITY CLASS. (of this report) UNCLASSIFIED	
		15a. DECLASSIFICATION/DOWNGRADING SCHEDULE	
16. DISTRIBUTION STATEMENT (of this Report) Distribution limited to U. S. Government agencies only; test and evaluation; statement applied in October 1977. Other requests for this document must be referred to AF Flight Dynamics Laboratory, (FBR), Wright-Patterson AFB, Ohio 45433.			
17. DISTRIBUTION STATEMENT (of the abstract entered in Block 20, if different from Report)			
18. SUPPLEMENTARY NOTES			
19. KEY WORDS (Continue on reverse side if necessary and identify by block number) Buckling constraints Cylindrical Shell Discrete Stiffeners Orthogonal Stiffeners Weight Optimization			
20. ABSTRACT (Continue on reverse side if necessary and identify by block number) The buckling equations for the orthogonally stiffened cylindrical shells under uniform axial compression and external pressure and with classical simply-supported boundary conditions are formulated by treating the stiffeners as discrete elements. By assuming identical and equally spaced stringers and identical and equally spaced rings, the buckling equations can be uncoupled into several sets of simpler and manageable equations for the symmetric and antisymmetric			

291 850

Handwritten signature

longitudinal modes and symmetric and antisymmetric circumferential modes. The uncoupled submatrices are further reduced by partitioning and substitution. Effort is made to preserve the sparseness of the matrices in order to use a special compact storage scheme. A method to compute the minimum eigenvalue for a large general eigenvalue problem, the Ritz iteration method combined with Chebyshev procedure, is developed and its accuracies are evaluated. Examples are performed and results are compared to other computational and experimental results available.

The minimum weight design for the simply-supported orthogonally stiffened cylindrical shell with smeared-out and discrete stiffeners subjected to axial compression is studied by a method of multipliers. The method for constraint function minimization proposed by Fletcher and Powell and the quasi-Newton method are used and compared. The difficulty in the formidably expensive computations of eigenvalues in the optimization process is circumvented by an approximate buckling formulation using extremely simple displacement functions. Expensive exact eigensolution is, however, performed for the optimized design variables to check the buckling load obtained by the approximate method. Seven design variables and fourteen inequality constraints are used for a design with a single stiffener size. Eleven design variables and twenty-one inequality constraints are used for a design with two stiffener sizes. The two designs are compared and discussed. From the calculations presented the design with two stiffener sizes can be lighter than the one with one stiffener size.

ACCESSION for		
NTIS	W	no
DDC	R	
UNANNOUNCED		
JUSTIFICATION		
BY _____		
DISTRIBUTION/AVAILABILITY CODES		
Dist.	is	SP-CIAL
B		

FOREWORD

This report was prepared by Dr. T. Y. Yang, Visiting Scientist in the Optimization Group, Analysis and Optimization Branch, Structural Mechanics Division, Air Force Flight Dynamics Laboratory (AFFDL/FBR), Air Force Wright Aeronautical Laboratories, Air Force Systems Command, Wright-Patterson Air Force Base, Ohio. This work was performed under Project Nr. 2307, "Research in Flight Vehicle Dynamics", Task Nr. 230705, "Basic Research in Structures and Dynamics".

This work was also performed under Contract F33615-76-C-3145 by T. Y. Yang, Professor of School of Aeronautics and Astronautics, Purdue University, West Lafayette, Indiana 47907.

The technical report was released by the Author in October 1977. The report covers work conducted from June 1976 through October 1977.

TABLE OF CONTENTS

<u>SECTION</u>	<u>PAGE</u>
I INTRODUCTION	1
II BUCKLING FORMULATIONS	5
1. Basic Assumptions	5
2. Total Potential Energy Expressions	5
3. Displacement Functions	7
4. Equilibrium Equations for Buckling Analysis	8
5. Equally Spaced and Identical Discrete Stringers and Rings	13
6. Further Consideration of Identical and Equally Spaced Discrete Stringers and Rings	16
III NUMERICAL METHOD FOR BUCKLING EQUATIONS	19
IV NUMERICAL RESULTS FOR BUCKLING ANALYSIS	23
1. Simply-Supported Cylinder with Many Stiffeners Under Uniform Axial Compression - By Both Smeared- out and Discrete Techniques	23
2. Simply-Supported Cylinder With One Ring and Four Stringers Under Uniform Axial Compression	24
3. Comparison With Experimental Results	28
(a) Cylinder With Eight Outer Stringers and Two Inner Rings Under External Pressure	30
(b) Cylinder With Eight Outer Stringers and Two Inner Rings Under Uniform Axial Compression	30
V WEIGHT, CONSTRAINTS, AND DESIGN VARIABLES	34

PRECEDING PAGE BLANK-NOT FILMED

TABLE OF CONTENTS (Continued)

<u>SECTION</u>	<u>PAGE</u>
VI A SIMPLIFIED BUCKLING FORMULATION	38
VII THEORY OF OPTIMIZATION	42
VIII TWO OPTIMUM WEIGHT DESIGN EXAMPLES	46
IX CONCLUDING REMARKS	53
REFERENCES	57

LIST OF ILLUSTRATIONS

<u>FIGURE</u>	<u>PAGE</u>
1 A Cylindrical Shell With Smeared-out and Discrete Stiffeners.	6
2 (a) The Nonzero Elements in a Typical Buckling Matrix; (b) The Two Uncoupled Submatrices With Symmetric and Antisymmetric Longitudinal Modes; and (c) The Four Further Uncoupled Submatrices With Circumferentially Related Modes	17
3 Buckling Mode Shapes for Antisymmetric Circumferential Mode and (a) Mixed Longitudinal Modes ($\sigma_x = 4070$ psi; $k_m = 28$; $k_n = 6$; $n = 1, 2, \dots, 6$); (b) Symmetric Longitudinal Mode ($\sigma_x = 4068$ psi; $k_m = 15$; $k_n = 7$; $n = 4, 8, \dots, 28$).	26
4 Buckling Mode Shapes for Antisymmetric Longitudinal Mode and (a) Symmetric Circumferential Mode ($\sigma_x = 4068.4$ psi; $k_m = 15$; $k_n = 7$; $n = 2, 6, \dots, 26$); (b) Antisymmetric Circumferential Mode ($\sigma_x = 4068.1$ psi; $k_m = 14$; $k_n = 6$; $n = 2, 6, \dots, 22$).	27
5 Buckling Mode Shape for Simply-Supported Cylinder With One Ring and Four Stringers Under Axial Compression (Uniform Strain Assumption).	29
6 Buckling Mode Shape for Clamped Cylinder With Two Inner Rings and Eight Outer Stringers Under External Pressure.	31

LIST OF ILLUSTRATIONS (Continued)

<u>FIGURE</u>		<u>PAGE</u>
7	Buckling Mode Shape for Clamped Cylinder With Two Inner Rings and Eight Outer Stringers Under Axial Compression	33
8	Buckling Mode Shape for the Optimized Cylindrical Shell With Smeared-out and Discrete Stiffeners	50

LIST OF TABLES

<u>TABLE</u>	<u>PAGE</u>
1 COMPARISON OF CONVERGENCE.....	22
2 UNIFORM AXIAL BUCKLING LOAD P_x FOR EXAMPLE (1).....	23
3 THE BUCKLING STRESSES FOR THE DISCRETELY STIFFENED CYLINDER.....	25
4 WEIGHT MINIMIZATION USING THE SMEARED-OUT FORMULATION ($N_{x0} = 789.82$ lbs/in; $\sigma_y = 50$ ksi; 0.01 in. $\leq u_i \leq 10$ in., $i = 1, 2, \dots, 7$).....	47
5 WEIGHT MINIMIZATION USING SMEARED-OUT AND DISCRETE FORMULATIONS ($N_{x0} = 789.82$ lbs/in; $\sigma_y = 50$ ksi; 0.01 in. $\leq u_i \leq 10$ in. with $i = 1, 2, \dots, 11$; $n_s = 30$; $n_r = 5$).....	48
6 PROCESS OF THE WEIGHT MINIMIZATION BY THE FLETCHER- POWELL METHOD.....	51

LIST OF SYMBOLS

A	=	cross sectional area
a_1, a_2	=	spacings between longitudinal and circumferential smeared-out stiffeners, respectively
d_1, d_2	=	depths of the longitudinal and circumferential smeared-out stiffeners, respectively
d_s, d_r	=	depths of the discrete stringers and rings, respectively
E_s, E_r	=	Young's moduli of the discrete stringers and rings, respectively
h	=	thickness of the shell skin
h_{e1}, h_{e2}	=	equivalent thicknesses of the smeared-out longitudinal and circumferential stiffeners defined, respectively, as $d_1 t_1 / a_1$ and $d_2 t_2 (1/a_2 - 1/L)$
h_{es}, h_{er}	=	equivalent thicknesses of the discrete stringers and rings defined, respectively, as $A_s / 2\pi r$ and A_r / L
J	=	$\sum_{k=1}^n [1 - (192t/\pi^5 d) \tanh(\pi d/2t)] t^3 d/3$, torsional constant of the stiffener (Reference 42)
L	=	length of the cylindrical shell
m, n	=	longitudinal half-wave and circumferential full-wave numbers, respectively
n_s, n_r	=	number of discrete stringers and rings, respectively
N_x	=	uniform axial buckling load defined as $P_x / 2\pi r$
p	=	external buckling pressure
P_x	=	uniform axial buckling load
r	=	mean radius of the cylindrical shell skin
t_1, t_2	=	widths of the longitudinal and circumferential smeared-out stiffeners, respectively
t_s, t_r	=	widths of the discrete stringer and ring, respectively
u, v, w	=	displacement components in x, θ , and z directions, respectively
U_{mn}, V_{mn}, W_{mn}	=	amplitudes in the displacement functions

LIST OF SYMBOLS (Continued)

- x, θ, z = cylindrical coordinates shown in Fig. 1
 Z = $L^2(1-\nu^2)^{1/2}$ /hr, geometric parameter
 $\epsilon_1, \epsilon_2, \epsilon_{12}$ = direct and shearing strain components
 $\epsilon_x, \epsilon_\theta$ = longitudinal and circumferential strains in the shell skin, respectively
 $\epsilon_{x1}, \epsilon_{\theta 2}$ = strains of the longitudinal and circumferential smeared-out stiffeners, respectively
 $\epsilon_{xs}, \epsilon_{\theta r}$ = strains of the discrete stringers and rings, respectively
 ν = Poisson's ratio
 ρ = weight density
 σ = stresses with subscripts 1, 2, 12, x, θ , x1, $\theta 2$, xs, and θr having the same meanings as those used for strains ϵ
 $[x]$ = Gaussian symbol defined as the integer not greater than x and with the same sign as x
 $i_1 \equiv i_2 \pmod{i_3} = i_1$ being congruent to i_2 modulo i_3 , defined as $i_2 - [i_2/i_3]i_3$

SECTION I

INTRODUCTION

Since van der Neut (Reference 1) demonstrated the influence of eccentricity of stiffeners on the buckling strength of stiffened cylindrical shell in 1947, numerous papers on the buckling analysis of stiffened cylindrical shells using the smeared-out technique were published (References 2-10). Such studies were motivated by the structural efficiency and practical advantages of the wall-stiffening. Reference 3 showed that when the smeared-out method was used for cylinders with large number of stiffeners, good correlation between experimental and theoretical results in buckling load was obtained. However, this may not be the case for cylinders with small number of stiffeners.

MacNeal et al. (Reference 11) treated ring-stiffened cylindrical shells by considering rings as discrete elements. Wang and Lin (Reference 12) and Singer and Haftka (Reference 13) analyzed the buckling of cylindrical shells with discrete stringers and showed the differences in results between the smeared-out and the discrete methods.

Egle and Sewall (Reference 14) derived the frequency equations for the cylindrical shells with discrete stringers and rings. Useful information on circumferential modes, which are in common for both vibration and buckling problems, was given. Their numerical results were limited to the study of the effect of discrete stringers on natural frequencies. McDonald (Reference 15) solved a problem on the free vibration of stiffened cylindrical shells by considering rings as discrete elements.

Wang (Reference 16) performed the deformation and stress calculations for orthogonally stiffened cylinders under internal pressure by treating the stiffeners as separate elements. Soong (Reference 17) analyzed the general instability

of orthotropic stiffened cylinders with intermittently attached stiffeners by considering the discreteness of the stiffeners. The buckling patterns assumed were symmetric circumferential and symmetric longitudinal modes. The results calculated on the basis of those displacement functions for the cylindrical shells with many stiffeners agreed well with experimental data and smeared-out calculations.

In this report, the discreteness of the stiffeners is considered in the buckling analysis of orthogonally stiffened cylinders with classical simply supported edge conditions. It is shown that when all the stringers are identical and equally spaced, the buckling equations can be reduced to two sets of equations, one set yields the antisymmetric circumferential modes and the other yields the symmetric circumferential modes. Each set can then be uncoupled into several circumferentially related equations. It is also shown that when all rings are identical and equally spaced, the buckling equations can be reduced to two sets of equations, one set yields the antisymmetric longitudinal modes and the other yields the symmetric longitudinal modes. The uncoupled submatrices are further reduced by partitioning and substitution. Effort is made to preserve the sparseness of the matrices in order to save computing time and storage by using a special compact storage scheme (Reference 20).

The large sets of general eigenvalue buckling equations are solved by the Ritz iteration method combined with Chebyshev procedure (Reference 18). The accuracy and efficiency of the method are evaluated through an example.

Examples of buckling predictions for discretely stiffened cylinders are performed and results are compared with available analytical and experimental solutions (Reference 19).

The problems of minimum weight design of stiffened cylindrical shell under buckling constraints have long been of interest to the aerospace structural

designers. The studies of such problems have been extensive (References 21-37).

Before 1967, the studies were based on the assumption of simultaneous failure modes and the optimization was achieved by parametric studies (References 21-23). The structural syntheses for the subject problems were performed, among others, by Kicher (Reference 24), Schmit, Morrow, and Kicher (Reference 25), and Pappas and Amba-Rao (Reference 28). Kicher treated the problem by using the constrained gradient method. Schmit, Morrow, and Kicher applied a Fiacco-McCormick-type penalty function formulation to transform the basic inequality constrained minimization problem into a sequence of unconstrained minimization problem. Pappas and Amba-Rao used a direct search algorithm with an interior-exterior penalty function formulation.

Thornton performed the synthesis of stiffened conical shells using the exterior penalty function method with least square approximation (Reference 32). Kunoo and Yang carried out the minimum weight design of cylindrical shells with orthogonal stiffeners subjected to uniform axial compressive or bending load by the method of steepest descent (Reference 37).

Hofmeister and Felton showed that the waffle plate with multiple rib sizes compared more favorably to sandwich plates than those with a single stiffener size (References 38-39).

In all the references (References 21-37) concerned with the weight optimization of the stiffened shells, it appears that all the buckling predictions were based on the formulations using smeared-out technique to treat the stiffeners. The main reason for not using discrete design and discrete formulation is that they result in large sets of eigenvalue equations that are extremely expensive to solve repeatedly during optimization.

In this report, the exact buckling formulations for the cylindrical shells with discrete stiffeners are derived. By assuming equally spaced and identical

discrete stringers and rings, the buckling formulations can be uncoupled into simpler ones based on their associated mode shapes. Then following some matrix partitioning and reduction, some efficient use of matrix sparsities, and the use of efficient eigenvalue solution procedures, the huge sets of eigenvalue equations can be reduced and become manageable. It is demonstrated in a typical example of cylinder with discrete stiffeners that approximately 400 seconds of central processing time are required for computing one lowest eigenvalue by a CDC 6500 computer. Such problem was governed by 750 eigenvalue equations in the original coupled formulation. The computing time of 400 seconds is, however, still formidably long in the minimum weight design where repeated computations of the lowest eigenvalues are required.

To circumvent this difficulty, it is suggested here to assume extremely simple displacement functions in the buckling formulation. With such simplicity, the computing time required for repeated eigenvalue computations in the optimization process becomes small. To ensure that the optimized design is feasible, the exact buckling load based on the exact discrete formulation is finally computed using the optimized design variables to check the buckling load obtained by the approximate method.

A method of multipliers recently developed by Schuldt (Reference 40) for mathematical programming problems is extended to the present structural problems for efficient minimum weight design.

Two design examples, one with the smeared-out and one with both the smeared-out and the discrete stiffeners, are performed to illustrate the present simplified buckling analysis method and the method of multipliers for optimization.

SECTION II
BUCKLING FORMULATIONS

1. BASIC ASSUMPTIONS

For the shell skin, it is assumed that the Kirchhoff and Love assumptions for thin elastic shell hold.

For the stiffeners, the following assumptions are made.

(a) The shell is integrally stiffened by longitudinal stringers and circumferential rings for both smeared-out and discrete types.

(b) The smeared-out stiffeners are thin and deep such that the uniaxial stress condition prevails and the torsional stiffness can be neglected.

2. TOTAL POTENTIAL ENERGY EXPRESSIONS

The total potential energy for the system as shown in Figure 1 is defined as

$$\Pi = U_1 + U_2 + U_3 + U_4 - W_1 - W_2 - W_3 \quad (1)$$

where U_1 is the strain energy for the shell skin; U_2 is the strain energy for the smeared-out orthogonal stiffeners; U_3 and U_4 are the strain energies for the discrete stringers and rings, respectively; W_1 , W_2 , and W_3 are the potential energies due to the middle-surface load for the shell with the smeared-out stiffeners, the discrete stringers, and the discrete rings, respectively.

The strain energy expressions written in terms of strains are available collectively in, for example, References 2, 10, and 14. These expressions can be derived in terms of displacements by using the following strain-displacement relations

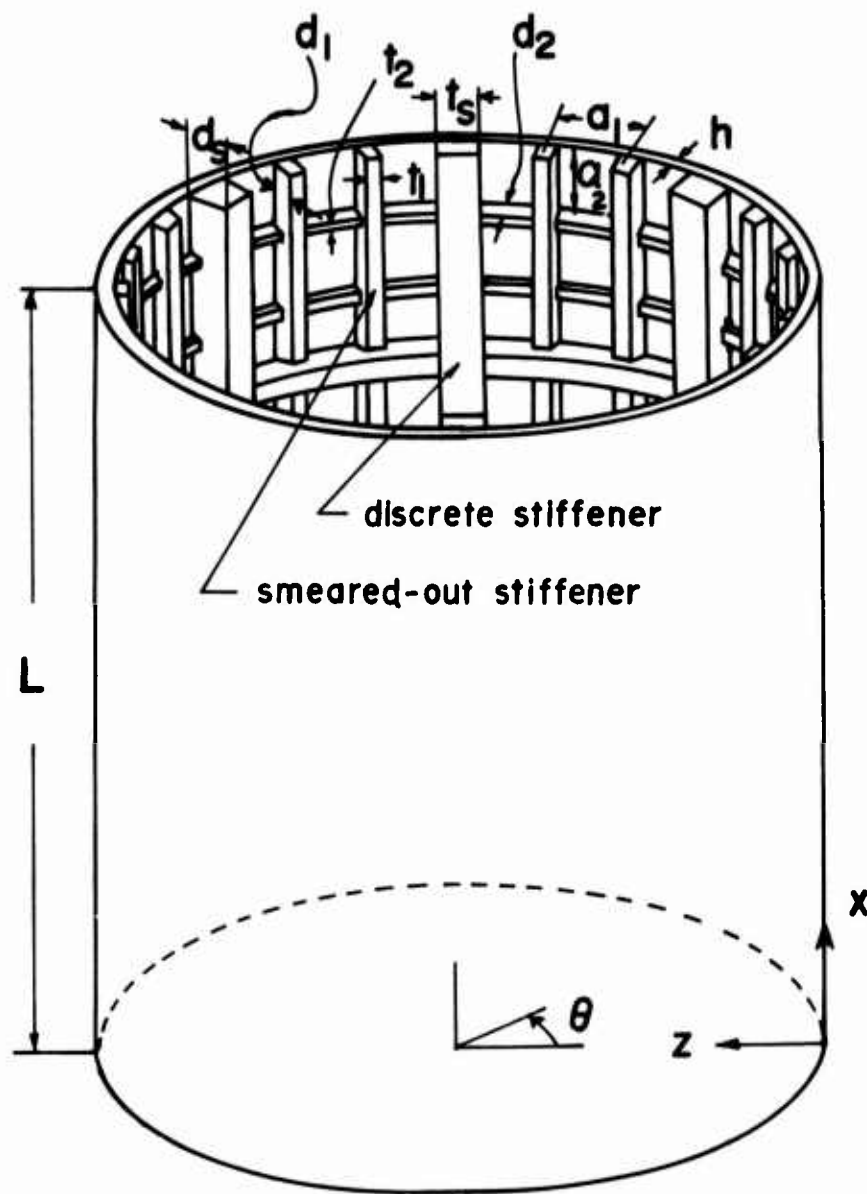


Figure 1 A Cylindrical Shell With Smeared-out and Discrete Orthogonal Stiffeners.

$$\begin{aligned}
\epsilon_1 &= u_{,x} - zw_{,xx} \\
\epsilon_2 &= v_{,\theta}/r - w/r - z(v_{,\theta} + w_{,\theta\theta})/r^2 \\
\epsilon_{12} &= v_{,x} + u_{,\theta}/r - 2z(w_{,x\theta} + v_{,x}/2)/r
\end{aligned} \tag{2}$$

It is noted that the terms $zv_{,\theta}/r^2$ and $zv_{,x}/r$ are neglected if Donnell type theory is used.

The potential energy versus displacement expressions take the following forms,

$$\begin{aligned}
W_1 &= \int_0^L \int_0^{2\pi} \left\{ (u_{,x} + \frac{1}{2} v_{,x}^2 + \frac{1}{2} w_{,x}^2) (\sigma_x h + \sigma_{x1} h_{e1}) \right. \\
&\quad \left. + \left(\frac{1}{r} v_{,\theta} - \frac{1}{r} w_{,r} + \frac{1}{2} \frac{1}{r^2} u_{,\theta}^2 + \frac{1}{2} \frac{1}{r^2} w_{,\theta}^2 \right) (\sigma_\theta h + \sigma_{\theta 2} h_{e2}) \right\} r d\theta dx \tag{3}
\end{aligned}$$

$$W_2 = \sum_{k=1}^{n_s} \int_0^L \sigma_{xs} A_{s_k} (u_{,x} + \frac{1}{2} w_{,x}^2)_{\theta=\theta_k} dx \tag{4}$$

$$W_3 = \sum_{k=1}^{n_r} \int_0^{2\pi} \sigma_{\theta r} A_{r_k} \left(\frac{1}{r} v_{,\theta} - \frac{w}{r} + \frac{1}{2} \frac{1}{r^2} u_{,\theta}^2 + \frac{1}{2} \frac{1}{r^2} w_{,\theta}^2 \right)_{x=x_k} r d\theta \tag{5}$$

3. DISPLACEMENT FUNCTIONS

The displacement functions which satisfy the classical simply-supported boundary conditions that $w = M_x = N_x = v = 0$ at $x = 0$ and L may be represented as

$$u = \sum_{m=1}^{k_m'} \frac{U_{m0}''}{2} \cos \frac{m\pi x}{L} + \sum_{m=1}^{k_m'} \sum_{n=1}^{k_n'-1} (U_{mn}' \sin n\theta + U_{mn}'' \cos n\theta) \cos \frac{m\pi x}{L}$$

$$\begin{aligned}
C'_{22}(i,j) = & \delta_{ij} \left[\left\{ \frac{Eh}{1-\nu^2} + \frac{Eh^3}{12(1-\nu^2)} \frac{1}{r^2} \right\} \left\{ \left(\frac{n}{r} \right)^2 + \frac{1-\nu}{2} \left(\frac{m\pi}{L} \right)^2 \right\} \right. \\
& + \frac{E_2 t_2 d_2}{a_2} \left(\frac{n}{r} \right) \left\{ 1 \mp \frac{(d_2+h)}{r} + \left(-\frac{d_2^2}{3} + \frac{d_2 h}{2} + \frac{h^2}{4} \right) \frac{1}{r^2} \right\} \\
& + \delta_{n_i n_j} \frac{2}{L} \left(\frac{n}{r} \right)^2 \sum_{k=1}^{n_r} (E_{r_k} A_{r_k} - \frac{2\bar{Z}_{r_k} A_{r_k} E_{r_k}}{r} + \frac{E_{r_k} I_{r_k}}{r^2} \\
& \times \sin \frac{m_i \pi X_k}{L} \sin \frac{m_j \pi X_k}{L}
\end{aligned}$$

$$\begin{aligned}
C'_{32}(i,j) = & \delta_{ij} \left(\frac{n}{r} \right) \frac{1}{r} \left[\frac{Eh}{1-\nu^2} + \frac{Eh^3}{12(1-\nu^2)} \left\{ \left(\frac{n}{r} \right)^2 + \left(\frac{m\pi}{L} \right)^2 \right\} + \frac{E_2 t_2 d_2}{a_2} \left\{ 1 \right. \right. \\
& \left. \left. \mp \frac{d_2+h}{2r} (1+n^2) + \left(-\frac{d_2^2}{3} + \frac{d_2 h}{2} + \frac{h^2}{4} \right) \left(\frac{n}{r} \right)^2 \right\} \right] + \delta_{n_i n_j} \frac{2}{rL} \left(\frac{n}{r} \right) \\
& \times \sum_{k=1}^{n_r} E_{r_k} \left\{ A_{r_k} - (1+n^2) \frac{\bar{Z}_{r_k} A_{r_k}}{r} + \left(\frac{n}{r} \right)^2 I_{r_k} \right\} \sin \frac{m_i \pi X_k}{L} \sin \frac{m_j \pi X_k}{L}
\end{aligned}$$

$$\begin{aligned}
C'_{33}(i,j) = & \delta_{ij} \left[\frac{Eh}{1-\nu^2} \frac{1}{r^2} + \frac{Eh^3}{12(1-\nu^2)} \left\{ \left(\frac{m\pi}{L} \right)^2 + \left(\frac{n}{r} \right)^2 \right\} + \frac{E_2 t_2 d_2}{a_2} \left\{ \frac{1}{r^2} \right. \right. \\
& \left. \left. \mp \frac{d_2+h}{r} \left(\frac{n}{r} \right)^2 + \left(\frac{n}{r} \right)^4 \left(-\frac{d_2^2}{3} + \frac{d_2 h}{2} + \frac{h^2}{4} \right) \right\} + \frac{E_1 t_1 d_1}{a_1} \left(-\frac{d_1^2}{3} + \frac{d_1 h}{2} \right. \right. \\
& \left. \left. + \frac{h^2}{4} \right) \left(\frac{m\pi}{L} \right)^4 \right] + \delta_{m_i m_j} \frac{1}{\pi r} \left(\frac{m\pi}{L} \right)^2 \sum_{k=1}^{n_s} \{ E_{s_k} I_{s_k} \left(\frac{m\pi}{L} \right)^2 \\
& \times \sin n_i \theta_k \sin n_j \theta_k + \frac{G_{s_k} J_{s_k}}{r^2} n_i n_j \cos n_i \theta_k \cos n_j \theta_k \} \\
& + \delta_{n_i n_j} \frac{2}{rL} \sum_{k=1}^{n_r} \left[E_{r_k} \left\{ -\frac{A_{r_k}}{r} - 2\bar{Z}_{r_k} A_{r_k} \left(\frac{n}{r} \right)^2 + I_{r_k} n \left(\frac{n}{r} \right)^3 \right\} \right. \\
& \times \sin \frac{m_i \pi X_k}{L} \sin \frac{m_j \pi X_k}{L} + G_{r_k} J_{r_k} \left(\frac{n}{r} \right)^2 \left(\frac{m_i \pi}{L} \right) \left(\frac{m_j \pi}{L} \right) \\
& \left. \times \cos \frac{m_i \pi X_k}{L} \cos \frac{m_j \pi X_k}{L} \right]
\end{aligned}$$

$$C_{11}''(i,j) = \delta_{ij} \left[\frac{Eh}{1-\nu^2} \left\{ \left(\frac{m\pi}{L} \right)^2 + \frac{1-\nu}{2} \left(\frac{n}{r} \right)^2 \right\} + \frac{E_1 t_1 d_1}{a_1} \left(\frac{m\pi}{L} \right)^2 \right] \\ + \delta_{m_i m_j} \frac{1}{\pi r} \left(\frac{m\pi}{L} \right)^2 \sum_{k=1}^{n_s} A_{S_k} E_{S_k} \cos n_i \theta_k \cos n_j \theta_k$$

$$C_{21}''(i,j) = \delta_{ij} \left[- \frac{Eh}{1-\nu^2} \frac{1+\nu}{2} \left(\frac{m\pi}{L} \right) \left(\frac{n}{r} \right) \right]$$

$$C_{31}''(i,j) = \delta_{ij} \left[\frac{Eh}{1-\nu^2} \frac{\nu}{r} \left(\frac{m\pi}{L} \right) + \frac{E_1 d_1 (d_1+h) t_1}{2a_1} \left(\frac{m\pi}{L} \right)^3 \right] \\ - \delta_{m_i m_j} \frac{1}{\pi r} \left(\frac{m\pi}{L} \right)^3 \sum_{k=1}^{n_s} \bar{z}_{S_k} A_{S_k} E_{S_k} \cos n_i \theta_k \cos n_j \theta_k$$

$$C_{22}''(i,j) = \delta_{ij} \left[\left\{ \frac{Eh}{1-\nu^2} + \frac{Eh^3}{12(1-\nu^2)} \frac{1}{r^2} \right\} \left\{ \left(\frac{n}{r} \right)^2 + \frac{1-\nu}{2} \left(\frac{m\pi}{L} \right)^2 \right\} \right. \\ \left. + \frac{E_2 d_2 t_2}{a_2} \left(\frac{n}{r} \right)^2 \left\{ 1 + \frac{d_2+h}{r} + \left(\frac{d_2^2}{3} + \frac{d_2 h}{2} + \frac{h^2}{4} \right) \frac{1}{r^2} \right\} \right] \\ + \delta_{n_i n_j} \frac{2}{L} \left(\frac{n}{r} \right)^2 \sum_{k=1}^{n_r} E_{r_k} \left\{ A_{r_k} - \frac{2\bar{z}_{r_k} A_{r_k}}{r} + \frac{I_{r_k}}{r^2} \right\} \sin \frac{m_i \pi x_k}{L} \sin \frac{m_j \pi x_k}{L}$$

$$C_{32}''(i,j) = \delta_{ij} \left(\frac{n}{r} \right) \frac{1}{r} \left[\frac{Eh}{1-\nu^2} + \frac{Eh^3}{12(1-\nu^2)} \left\{ \left(\frac{n}{r} \right)^2 + \left(\frac{m\pi}{L} \right)^2 \right\} - \frac{E_2 t_2 d_2}{a_2} \right. \\ \left. \left\{ 1 + \frac{d_2+h}{2r} (1+n^2) + \left(\frac{d_2^2}{3} + \frac{d_2 h}{2} + \frac{h^2}{4} \right) \left(\frac{n}{r} \right)^2 \right\} \right] \\ - \delta_{n_i n_j} \frac{2}{rL} \left(\frac{n}{r} \right) \sum_{k=1}^{n_r} E_{r_k} \left\{ A_{r_k} - (1+n^2) \frac{\bar{z}_{r_k} A_{r_k}}{r} + \left(\frac{n}{r} \right)^2 I_{r_k} \right\} \\ \times \sin \frac{m_i \pi x_k}{L} \sin \frac{m_j \pi x_k}{L}$$

$$C_{33}''(i,j) = \delta_{ij} \left[\frac{Eh}{1-\nu^2} \frac{1}{r^2} + \frac{Eh^3}{12(1-\nu^2)} \left\{ \left(\frac{m\pi}{L} \right)^2 + \left(\frac{n}{r} \right)^2 \right\}^2 + \frac{E_2 t_2 d_2}{a_2} \left(\frac{1}{r^2} \right) \right]$$

$$\begin{aligned}
& \bar{r} \left\{ \frac{d_2+h}{r} \left(\frac{n}{r}\right)^2 + \left(\frac{n}{r}\right)^4 \left(\frac{d_2^2}{3} + \frac{d_2 h}{2} + \frac{h^2}{4}\right) \right\} \\
& + \frac{E_1 t_1 d_1}{a_1} \left(\frac{d_1^2}{3} + \frac{d_1 h}{2} + \frac{h^2}{4}\right) \left(\frac{m\pi}{L}\right)^4 \Big] \\
& + \delta_{m_i m_j} \frac{1}{\pi r} \left(\frac{m\pi}{L}\right)^2 \sum_{k=1}^{n_s} \{E_{S_k} I_{S_k} \left(\frac{m\pi}{L}\right)^2 \cos n_i \theta_k \cos n_j \theta_k \\
& + \frac{G_{S_k}^J J_{S_k}}{r^2} n_i n_j \sin n_i \theta_k \sin n_j \theta_k \} \\
& + \delta_{n_i n_j} \frac{2}{rL} \sum_{k=1}^{n_r} \left[E_{r_k} \left\{ \frac{A_{r_k}}{r} - 2 \bar{z}_{r_k} A_{r_k} \left(\frac{n}{r}\right)^2 + I_{r_k} n \left(\frac{n}{r}\right)^3 \right\} \right. \\
& \times \sin \frac{m_i \pi X_k}{L} \sin \frac{m_j \pi X_k}{L} + G_{r_k}^J J_{r_k} \left(\frac{n}{r}\right)^2 \left(\frac{m_i \pi}{L}\right) \left(\frac{m_j \pi}{L}\right) \\
& \left. \times \cos \frac{m_i \pi X_k}{L} \cos \frac{m_j \pi X_k}{L} \right]
\end{aligned}$$

$$C_{11}'''(i,j) = \delta_{m_i m_j} \frac{1}{\pi r} \left(\frac{m\pi}{L}\right)^2 \sum_{k=1}^{n_s} A_{S_k} E_{S_k} \sin n_i \theta_k \cos n_j \theta_k$$

$$C_{21}'''(i,j) = C_{12}'''(i,j) = C_{22}'''(i,j) = C_{32}'''(i,j) = C_{23}'''(i,j) = 0$$

$$C_{13}'''(i,j) = C_{31}'''(i,j) = -\delta_{m_i m_j} \frac{1}{\pi r} \left(\frac{m\pi}{L}\right)^3 \sum_{k=1}^{n_s} \bar{z}_{S_k} A_{S_k} E_{S_k} \sin n_i \theta_k \cos n_j \theta_k$$

$$\begin{aligned}
C_{33}'''(i,j) &= \delta_{m_i m_j} \frac{1}{\pi r} \left(\frac{m\pi}{L}\right)^2 \sum_{k=1}^{n_s} \{E_{S_k} I_{S_k} \left(\frac{m\pi}{L}\right)^2 \sin n_i \theta_k \cos n_j \theta_k \\
&- \frac{G_{S_k}^J J_{S_k}}{r^2} n_i n_j \sin n_i \theta_k \cos n_j \theta_k \}
\end{aligned}$$

$$D_{33}^i(i,j) = \delta_{ij} \left\{ (\sigma_x h + \sigma_{x1} h e_1) \left(\frac{m\pi}{L}\right)^2 + (\sigma_\theta h + \sigma_{\theta 2} h e_2) \left(\frac{n}{r}\right)^2 \right\}$$

$$\begin{aligned}
& + \delta_{m_i m_j} \frac{1}{\pi r} \left(\frac{m\pi}{L}\right)^2 \sum_{k=1}^{n_s} \sigma_{xs} A_{S_k} \sin n_i \theta_k \sin n_j \theta_k \\
& + \delta_{n_i n_j} \frac{2}{L} \left(\frac{n}{r}\right)^2 \sum_{k=1}^{n_r} \sigma_{\theta r} A_{r_k} \sin \frac{m_i \pi X_k}{L} \sin \frac{m_j \pi X_k}{L} \\
D''_{33}(i, j) & = \delta_{ij} \{ (\sigma_x h + \sigma_{x1} h_{e1}) \left(\frac{m\pi}{L}\right)^2 + (\sigma_\theta h + \sigma_{\theta 2} h_{e2}) \left(\frac{n}{r}\right)^2 \} \\
& + \delta_{m_i m_j} \frac{1}{\pi r} \left(\frac{m\pi}{L}\right)^2 \sum_{k=1}^{n_s} \sigma_{xs} A_{S_k} \cos n_i \theta_k \cos n_j \theta_k \\
& + \delta_{n_i n_j} \frac{2}{L} \left(\frac{n}{r}\right)^2 \sum_{k=1}^{n_r} \sigma_{\theta r} A_{r_k} \sin \frac{m_i \pi X_k}{L} \sin \frac{m_j \pi X_k}{L} \\
D'''_{33}(i, j) & = \delta_{m_i m_j} \frac{1}{\pi r} \left(\frac{m\pi}{L}\right)^2 \sum_{k=1}^{n_s} \sigma_{xs} A_{S_k} \sin n_i \theta_k \cos n_j \theta_k \quad (8)
\end{aligned}$$

As to the double signs, the upper and lower ones are for the inner and outer stiffened shells, respectively. The Kronecker delta function is defined as $\delta_{ij} = 0$ if $i \neq j$ and $\delta_{ij} = 1$ if $i = j$. For the matrix elements with subscripts 1 and 2, it is defined that

$$\begin{aligned}
m & = m_i = [i/(k_m' + 1)] + 1; & m_j & = [j/(k_m' + 1)] + 1 \\
n & = n_i = i - [i/(k_m' + 1)]; & n_j & = j - [j/(k_m' + 1)] \quad (9)
\end{aligned}$$

For the rest of the matrix elements, Eq. (9) also applies except that k_m' is replaced by k_m .

The order of the matrices in Eqs. (7) is $(4k_m' k_n' + 2k_m k_n)$. The submatrices \tilde{C}''' and \tilde{D}''' are functions of the properties of the discrete stringers only. If there is no stringers, Eqs. (7) reduce to two sets of equations which result in the same buckling load but two circumferential modes with 90° phase difference.

The uniform axial load and uniform external pressure are considered here. They are related to the internal stresses by using the assumption of either uniform

stresses or uniform strains in the system.

The stresses based on the uniform stress assumption are

$$\sigma_x = N_x / (h + h_{es} + h_{e1}) \quad \text{and} \quad \sigma_\theta = pr / (h + h_{er} + h_{e2}) \quad (10)$$

The stresses based on the uniform strain assumption are

$$\left\{ \begin{array}{l} \sigma_x = \{N_x(H_2 + H_r + 1) + vpr(H_1 + H_s)\} / hH \\ \sigma_\theta = \{vN_x(H_2 + H_r) + pr(H_1 + H_s + 1)\} / hH \\ \sigma_{x1} = [N_x\{(H_2 + H_r)(1 - v^2) + 1\} - vpr] / hH \\ \sigma_{\theta 2} = [-vN_x + pr\{(H_1 + H_s)(1 - v^2) + 1\}] / hH \\ \sigma_{xs} = E_s[N_x\{(H_2 + H_r)(1 - v^2) + 1\} - vpr] / EhH \\ \sigma_{\theta r} = E_r[-vN_x + pr\{(H_1 + H_s)(1 - v^2) + 1\}] / EhH \end{array} \right. \quad (11)$$

where $H = (H_1 + H_s + 1)(H_2 + H_r + 1) - v^2(H_1 + H_s)(H_2 + H_r)$; $H_1 = h_{e1}/h$; $H_2 = h_{e2}/h$; $H_s = E_s h_{es} / Eh$; and $H_r = E_r h_{er} / Eh$.

The axial load and external pressure have the relation that $N_x = pr/2$.

5. EQUALLY SPACED AND IDENTICAL DISCRETE STRINGERS AND RINGS

If the stringers are identical in size, the matrix elements with triple primes in Eqs. (7) include a common term,

$$L_{n_i n_j} = \sum_{k=1}^{n_s} \sin n_i \theta_k \cos n_j \theta_k \quad (12)$$

For equally spaced stringers, $\theta_k = 2\pi k/n_s$ and Eq. (12) becomes

$$L_{n_i n_j} = \frac{1}{2} \sum_{k=1}^{n_s} \sin \frac{2\pi(n_i - n_j)}{n_s} k + \frac{1}{2} \sum_{k=1}^{n_s} \sin \frac{2\pi(n_i + n_j)}{n_s} k = L'_{n_i n_j} + L''_{n_i n_j} \quad (13)$$

where $L'_{n_i n_j} = L''_{n_i n_j} = 0$ if $n_i - n_j \equiv 0 \pmod{n_s}$ and $n_i + n_j \equiv 0 \pmod{n_s}$. However, if $n_i - n_j \not\equiv 0 \pmod{n_s}$ and $n_i + n_j \not\equiv 0 \pmod{n_s}$, one obtains (Reference 41)

$$\begin{cases} L'_{n_i n_j} = \frac{1}{2} \sin \frac{\pi(n_i - n_j)(n_s + 1)}{n_s} \sin(n_i - n_j)\pi \operatorname{cosec} \frac{n_i - n_j}{n_s} \pi = 0 \\ L''_{n_i n_j} = \frac{1}{2} \sin \frac{\pi(n_i + n_j)(n_s + 1)}{n_s} \sin(n_i + n_j)\pi \operatorname{cosec} \frac{n_i + n_j}{n_s} \pi = 0 \end{cases} \quad (14)$$

Thus it is shown that for the case of identical and equally spaced stringers, the submatrix elements with triple primes in Eqs. (7) vanish. Eqs. (7) are thus uncoupled into two sets of equations. One set is related to the amplitudes U' , V' , and W' and yields the antisymmetric circumferential buckling modes. The other is related to the amplitudes U'' , V'' , and W'' and yields the symmetric circumferential buckling modes.

The elements in the submatrices with single and double primes contain two common terms

$$M_{n_i n_j} = \sum_{k=1}^{n_s} \cos n_i \theta_k \cos n_j \theta_k \quad \text{and} \quad N_{n_i n_j} = \sum_{k=1}^{n_s} \sin n_i \theta_k \sin n_j \theta_k \quad (15)$$

Using the similar procedures as used in deriving Eqs. (13 and 14), Eq. (15) becomes

$$M_{n_i n_j} = M'_{n_i n_j} + M''_{n_i n_j} \quad \text{and} \quad N_{n_i n_j} = N'_{n_i n_j} - N''_{n_i n_j} \quad (16)$$

where

$$\begin{cases} M'_{n_i n_j} = N'_{n_i n_j} = 0 & \text{if} & n_i - n_j \not\equiv 0 \pmod{n_s} \\ M''_{n_i n_j} = N''_{n_i n_j} = n_s/2 & \text{if} & n_i - n_j \equiv 0 \pmod{n_s} \\ M'_{n_i n_j} = N'_{n_i n_j} = 0 & \text{if} & n_i + n_j \not\equiv 0 \pmod{n_s} \\ M''_{n_i n_j} = N''_{n_i n_j} = n_s/2 & \text{if} & n_i + n_j \equiv 0 \pmod{n_s} \end{cases} \quad (17)$$

For identical and equally spaced rings, the buckling equations (7) include the following terms,

$$\begin{cases} Q_{m_i m_j} = \sum_{k=1}^{n_r} \cos \frac{m_i \pi X_k}{L} \cos \frac{m_j \pi X_k}{L} \\ R_{m_i m_j} = \sum_{k=1}^{n_r} \sin \frac{m_i \pi X_k}{L} \sin \frac{m_j \pi X_k}{L} \end{cases} \quad \text{with } X_k = kL/(n_r + 1) \quad (18)$$

Similar derivations give

$$Q_{m_i m_j} = Q'_{m_i m_j} + Q''_{m_i m_j} \quad \text{and} \quad R_{m_i m_j} = Q'_{m_i m_j} - Q''_{m_i m_j} \quad (19)$$

where

$$Q'_{m_i m_j} = \frac{1}{2} \cos \frac{\pi}{2} (m_i - m_j) \sin \frac{\pi}{2} \frac{n_r (m_i - m_j)}{n_r + 1} \operatorname{cosec} \frac{\pi}{2} \frac{(m_i - m_j)}{(n_r + 1)}$$

If $m_i - m_j \not\equiv 0 \pmod{2n_r + 2}$ (20)

$$Q'_{m_i m_j} = n_r/2 \quad \text{if } m_i - m_j \equiv 0 \pmod{2n_r + 2} \quad (21)$$

$$Q''_{m_i m_j} = \frac{1}{2} \cos \frac{\pi}{2} (m_i + m_j) \sin \frac{\pi}{2} \frac{n_r (m_i - m_j)}{n_r + 1} \operatorname{cosec} \frac{\pi}{2} \frac{(m_i - m_j)}{(n_r + 1)}$$

If $m_i + m_j \not\equiv 0 \pmod{2n_r + 2}$ (22)

$$Q''_{m_i m_j} = n_r/2 \quad \text{if } m_i + m_j \equiv 0 \pmod{2n_r + 2} \quad (23)$$

Further examination of Eqs. (20) to (23) reveals that if $m_i - m_j \not\equiv 0 \pmod{2}$ and $m_i + m_j \not\equiv 0 \pmod{2}$,

$$Q_{m_i m_j} = R_{m_i m_j} = 0 \quad (24)$$

This simple conclusion leads to the uncoupling of the buckling equations (7) into two sets, one gives the symmetric longitudinal buckling modes and the other gives the antisymmetric longitudinal buckling modes.

The equations derived here involve no summations, the computation is thus greatly simplified.

6. FURTHER CONSIDERATION OF IDENTICAL AND EQUALLY SPACED DISCRETE STRINGERS AND RINGS

A typical stiffness matrix element in the buckling equations (7) may be written in the symbolic form

$$C(i,j) = \delta_{ij}A + \delta_{m_i m_j} (B N_{n_i n_j} + D M_{n_i n_j}) + \delta_{n_i n_j} (E Q_{m_i m_j} + F R_{m_i m_j}) \quad (25)$$

Eq. (25) indicates that odd numbers of m_i and the even numbers of m_j are not related. In other words, if a row in the buckling matrix corresponding to some odd number of m_i , then all the elements in that row that correspond to the even numbers of m_j are zero. For a sample case with two stringers ($n_s = 2$), the non-zero elements in the matrix are shown in Fig. 2a. By properly interchanging rows and columns in Fig. 2a, the uncoupled version of matrix is obtained and shown in Fig. 2b. Fig. 2b shows that the submatrix that corresponds to the odd numbers of m_i and m_j results in a symmetric longitudinal buckling mode, whereas the other submatrix that corresponds to the even numbers of m_i and m_j results in an antisymmetric longitudinal buckling mode.

Extending this idea to the circumferential buckling mode, Eqs. (16) can be reduced as follows

$$M_{n_i n_j} = N_{n_i n_j} = 0 \quad \text{if} \quad \begin{cases} n_i - n_j \not\equiv 0 \pmod{n_s} \\ n_i + n_j \not\equiv 0 \pmod{n_s} \end{cases} \quad (26)$$

Eqs. (26) indicate that if some row in the buckling matrix corresponds to n_i , then all the elements in that row that corresponds to the number n_j which satisfies $n_i - n_j \not\equiv 0 \pmod{n_s}$ and $n_i + n_j \not\equiv 0 \pmod{n_s}$ are zero. In other words, the

	11	12	13	14	21	22	23	24	31	32	33	34	41	42	43	44
11	x		x						x							
12		x		x						x						
13	x		x								x					
14		x		x								x				
21					x		x						x			
22						x		x						x		
23					x		x								x	
24						x		x								x
31	x								x		x					
32		x								x		x				
33			x						x		x					
34				x						x		x				
41					x								x		x	
42						x								x		x
43							x						x		x	
44								x						x		x

	11	12	13	14	31	32	33	34	21	22	23	24	41	42	43	44
11	x		x		x											
12		x		x		x										
13	x		x				x									
14		x		x				x								
31	x				x		x									
32		x				x		x								
33			x		x		x									
34				x		x		x								
21									x		x		x			
22										x		x		x		
23									x		x				x	
24										x		x				x
41									x				x		x	
42										x				x		x
43											x		x		x	
44												x		x		x

	11	13	31	33	12	14	32	34	21	23	41	43	22	24	42	44
11	x	x	x													
13	x	x		x												
31	x		x	x												
33		x	x	x												
12					x	x	x									
14					x	x		x								
32					x		x	x								
34						x	x	x								
21									x	x	x					
23									x	x		x				
41									x		x	x				
43										x	x	x				
22													x	x	x	
24													x	x		x
42													x		x	x
44														x	x	x

Figure 2 (a) The nonzero elements in a typical buckling matrix;
 (b) The two uncoupled submatrices with symmetric and antisymmetric longitudinal modes; and
 (c) The four further uncoupled submatrices with circumferentially related modes.

elements with n_i and n_j that satisfy $n_i - n_j \equiv 0 \pmod{n_s}$ and $n_i + n_j \equiv 0 \pmod{n_s}$ are not zero. For example, if $n_s = 8$, the elements that correspond to the combinations with $(n_i, n_j = 1, 7, 9, 15, 17, \dots)$, $(n_i, n_j = 2, 6, 10, 14, \dots)$, $(n_i, n_j = 3, 5, 11, 13, 19, 21, \dots)$, $(n_i, n_j = 4, 12, 20, 28, \dots)$, and $(n_i, n_j = 0, 8, 16, 24, 32, \dots)$ have non-zero values. These relations may be illustrated in Figs. 2a, 2b, and 2c for the case of $n_s = 2$.

These procedures can be summarized as follows. The whole set of buckling equations is first uncoupled into two sets: one related to the symmetric circumferential modes and the other related to the antisymmetric circumferential modes. Each of these two sets is then uncoupled into two sub-sets: one related to the symmetric longitudinal modes and the other related to the antisymmetric longitudinal modes. The lowest eigenvalue that comes from these four sub-sets is the buckling load of the whole system.

SECTION III
 NUMERICAL METHOD FOR BUCKLING EQUATIONS

As shown in Eq. (14), for the case of equally spaced and identical stringers, the buckling equations (7) can be reduced into two sets; one related to the anti-symmetric circumferential modes and the other related to the symmetric circumferential modes. Both sets, although different in content, can be described in the same symbolic form.

$$\left[\begin{array}{c} \left[\begin{array}{ccc} \tilde{c}_{11} & \tilde{c}_{12} & \tilde{c}_{13} \\ \tilde{c}_{21} & \tilde{c}_{22} & \tilde{c}_{23} \\ \tilde{c}_{31} & \tilde{c}_{32} & \tilde{c}_{33} \end{array} \right] - \left[\begin{array}{ccc} \tilde{0} & \tilde{0} & \tilde{0} \\ \tilde{0} & \tilde{0} & \tilde{0} \\ \tilde{0} & \tilde{0} & \tilde{D}_{33} \end{array} \right] \end{array} \right] \begin{Bmatrix} \tilde{U} \\ \tilde{V} \\ \tilde{W} \end{Bmatrix} = \begin{Bmatrix} \tilde{0} \\ \tilde{0} \\ \tilde{0} \end{Bmatrix} \quad (27)$$

In order to save computer storage and computing time by a special compact storage scheme, effort to preserve the original form of the sparseness of the buckling submatrices is made.

Through some manipulations, Eqs. (27) are reduced to

$$\tilde{B} \tilde{W} = \lambda \tilde{A} \tilde{W} \quad (28)$$

where

$$\begin{aligned} \tilde{A} = & \tilde{c}_{33} - \tilde{c}_{31} \tilde{c}_{11}^{-1} \tilde{c}_{12} \tilde{E}^{-1} \tilde{c}_{21} \tilde{c}_{11}^{-1} \tilde{c}_{13} + \tilde{c}_{31} \tilde{c}_{11}^{-1} \tilde{c}_{12} \tilde{E}^{-1} \tilde{c}_{23} \\ & - \tilde{c}_{31} \tilde{c}_{11}^{-1} \tilde{c}_{13} + \tilde{c}_{32} \tilde{E}^{-1} \tilde{c}_{21} \tilde{c}_{11}^{-1} \tilde{c}_{13} - \tilde{c}_{32} \tilde{E}^{-1} \tilde{c}_{23} \end{aligned} \quad (29)$$

$$\tilde{B} = \lambda \tilde{D}_{33}$$

$$\tilde{E} = \tilde{c}_{22} - \tilde{c}_{21} \tilde{c}_{11}^{-1} \tilde{c}_{12}$$

For uniform axial compression and external pressure, matrices \tilde{A} and \tilde{B} are both positive definite and symmetric. Because only the smallest eigenvalue λ is of interest, the Power method may be used. Unfortunately, for the present class of problems the eigenvalues are poorly separated and the convergence is slow.

An effective algorithm called Ritz iteration was developed by Rutishauser (Reference 18) for standard eigenvalue problem. It can be extended to solve the eigenvalue equations (28) via the following procedure.

Matrix \tilde{A} is first decomposed as the product of a lower triangular matrix \tilde{L} and its transpose \tilde{L}^T by means of Cholesky factorization. Eq. (28) can then be derived as

$$\tilde{L}^{-1} \tilde{B} (\tilde{L}^T)^{-1} \tilde{X} = \lambda \tilde{X} \quad \text{with } \tilde{X} = \tilde{L}^T \tilde{W} \quad (30)$$

Matrix \tilde{X} is the initial matrix in iteration, whose columns are assumed as orthonormal and the order of the matrix is $p \times q$ with p being the order of matrix \tilde{A} and $q \leq p$. The iterative procedure is described by a typical cycle from step $k-1$ to k .

$$(a) \quad \begin{cases} \tilde{P} = (\tilde{L}^T)^{-1} \tilde{X}_{k-1} & \text{or } \tilde{L}^T \tilde{P} = \tilde{X}_{k-1} \\ \tilde{Q} = \tilde{B} \tilde{P} \\ \tilde{Z}_k = \tilde{L}^{-1} \tilde{Q} & \text{or } \tilde{L} \tilde{Z}_k = \tilde{Q} \end{cases} \quad (31)$$

$$(b) \quad \tilde{G}_k = \tilde{Z}_k^T \tilde{Z}_k \quad (32)$$

(c) Solve for the eigenvalues of the $q \times q$ matrix \tilde{G}_k

$$(d) \quad \tilde{X}_k = \tilde{Z}_k \tilde{R}_k \tilde{D}_k^{-1} \quad (33)$$

where \tilde{R}_k is the matrix of eigenvectors of matrix \tilde{G}_k , and \tilde{D}_k is the diagonal matrix whose elements are the square roots of the eigenvalues of matrix \tilde{G}_k in decreasing order. The eigenvalues of Eq. (28) are calculated by the Rayleigh quotient formula

$$\lambda = 1 + \tilde{X}_k^T \tilde{L}^{-1} \tilde{B} (\tilde{L}^T)^{-1} \tilde{X}_k \quad (34)$$

and the associated eigenvectors are given by Eq. (30) as

$$\hat{W} = (\hat{L}^T)^{-1} \hat{\chi}_k \quad (35)$$

The convergence rate of this method is considerably improved over the Power Method. It is, however, still slow for the present problems because quite a few eigenvalues are very close to the minimum eigenvalue. Rutishauser also suggested that if Chebyshev iteration is used in addition to the iterative step (a) in Eq. (31) considerable improvement in convergence rate can be achieved, especially when convergence is slow.

The Chebyshev iteration is expressed as

$$\hat{\chi}_{h+1} = \frac{1}{e} \hat{L}^{-1} \hat{B} (\hat{L}^T)^{-1} \hat{\chi}_h - \hat{\chi}_h \quad (36)$$

$$\hat{\chi}_{h+i} = \frac{2}{e} \hat{L}^{-1} \hat{B} (\hat{L}^T)^{-1} \hat{\chi}_{h+i-1} - 2\hat{\chi}_{h+i-1} - \hat{\chi}_{h+i-2} \quad (i=2,3,\dots,j-1) \quad (37)$$

where e meets the condition that

$$\lambda_{q+1} \leq 2e \leq \lambda_q \quad (38)$$

The entire procedure applied here may be described in the following nine steps.

- (1) Choose a set of values in matrix $\hat{\chi}_0$ ($p \times q$).
- (2) Orthonormalize the columns in matrix $\hat{\chi}_0$ by the Gram-Schmidt orthogonalization process (Reference 43).
- (3) Start with $h = 0$ and $j = 2$.
- (4) Compute $j - 1$ steps of $\hat{\chi}_h$ values by using Eqs. (36) and (37).
- (5) Orthonormalize the columns of $\hat{\chi}_{h+j-1}$.
- (6) Perform one step of iteration as described in (a), (b), (c) and (d) with $k = h + j$.

(7) Determine j such that it satisfies the condition

$$j - 1 < \text{Arccosh}(10) / \text{Arccosh} \{ (\lambda_{11} - e) / e \} \quad (39)$$

(8) Check tolerance in the lowest eigenvalue between two current steps.

(9) Return to step (4).

This procedure was successfully applied to the present large eigenvalue equations which contain poorly separated eigenvalues. This method can also calculate the equal eigenvalues which may appear in the vibration problem.

The convergence characteristics of the Power Method, the Ritz Iteration Method, and the Ritz Iteration Method combined with Chebyshev procedure were studied through a numerical example. The example was derived from Eqs. (27) with $k_m = k'_m = 4$ and $k_n = k'_n = 8$. The matrix given by Eqs. (27) had an order of 96 which was reduced to 32 by using Eqs. (28). The results are summarized in Table 1. The Ritz iteration method with Chebyshev procedure appears to be most efficient among the methods compared. This method was used in the example studies.

Table 1. Comparison of Convergence

Method	Mode Number				CDC 6500 CP Time (sec.)	Iteration
	Lowest	2nd	3rd	4th		
Exact	1511.627	1544.382	1590.751	1772.99		
Power	1511.630				12.0	245
Ritz Iteration	1511.629	1544.393	1590.759	1797.46	7.3	30 x 4
Ritz + Chebyshev	1511.627	1544.382	1590.751	1778.94	4.5	22 x 4

SECTION IV
NUMERICAL RESULTS FOR BUCKLING ANALYSIS

1. SIMPLY-SUPPORTED CYLINDER WITH MANY STIFFENERS UNDER UNIFORM AXIAL
COMPRESSION - BY BOTH SMEARED-OUT AND DISCRETE TECHNIQUES

The first example was defined by the dimensions and properties that $E = 1.06 \times 10^7$ psi; $\nu = 1/3$; $a_1 = a_2 = 3$ in.; $d_1 = d_2 = 0.2$ in.; $t_1 = t_2 = 0.125$ in.; $h = 0.05$ in.; $r = 48$ in.; $L = 50$ in., and weight = 100 pounds. The results are given in Table 2.

Table 2. Uniform Axial Buckling Load P_x for Example (1)

Method	P_x (kips)	$P_x/2\pi r$ (lbs/in.)	σ_x (psi)	Mode Numbers	
				m	n
(1) Discrete	243.7	808.0	13891	6	17
(2) Discrete	241.7	801.3	13776	6	17
(3) Smeared-out	238.7	791.5	13597	6	17

In the discrete calculations, 16 rings and 100 stringers were used. The first discrete calculation was based on the displacement functions with 600 terms ($k_m = k_m' = 10$, $k_n = k_n' = 20$), an antisymmetric circumferential mode, and uniform strain distribution. The second discrete calculation was based on five antisymmetric circumferentially related modes and 24 symmetric longitudinal modes ($k_n = 5$ with $n = 17, 83, 117, 183, 217$; $k_m = 24$ with $m = 1, 3, 5, \dots, 47$) and uniform strain distribution. The smeared-out calculation was based on uniform stress assumption and the result agreed with that given in Reference 10. Table 2 serves to verify the correctness of the present discrete formulations and solution methods. Because the torsional stiffnesses of the stiffeners were neglected in the smeared-out calculation, the resulted buckling load should be slightly smaller than those obtained by the discrete calculations.

When the numbers of rings and stringers are large, the buckling loads obtained by using uniform strain and uniform stress assumptions should be close. The first discrete computation was also performed by using the uniform stress assumption, a buckling load of 245.7 kips was obtained. Since the uniform strain assumption introduces circumferential tensions in the rings which produce compressive stresses in the skin, it always yields lower buckling load than the uniform stress assumption.

If the stiffeners in this example are neglected, the buckling stress σ_x for the monocoque cylinder becomes 6750 psi. The tremendous strengthening effect due to a large number of stiffeners is seen.

2. SIMPLY-SUPPORTED CYLINDER WITH ONE RING AND FOUR STRINGERS UNDER UNIFORM AXIAL COMPRESSION

The geometry and the material parameters of the second examples are defined as: $\nu = 1/3$; $h = 0.03$ in.; $r = 48$ in.; $L = 50$ in.; $d_s = d_r = 1.3196$ in.; $t_s = t_r = 0.8248$ in.; $Z = 1637$; and weight = 100 pounds. The buckling stresses computed by using the uniform stress assumption and either symmetric or antisymmetric circumferential mode are given in Table 3.

The converged buckling stress is 4070 psi. Table 3 reveals that one should not be prejudiced against the u and v functions by using more terms in the w function.

The buckling calculation was then performed by assuming uniform stress and either symmetric or antisymmetric circumferential mode, either symmetric ($m = 1, 3, \dots, 2k_m + 1$) or antisymmetric ($m = 2, 4, \dots, 2k_m$) longitudinal modes, and circumferentially related modes. The results for buckling stresses and mode shapes are shown in Figs. 3a, 3b, 4a, and 4b, respectively. The mode shapes were plotted by the Gould 4800 electrostatic printer. The four mode shapes in the figures are quite

Table 3. The Buckling Stresses For The Discretely Stiffened Cylinder.

Antisymmetric circumferential mode

k_m	k_n	k_m	k_n	No. of terms	Buckling Stress σ_x (lbs/in ²)	Relative Error	Iteration Number	CDC-6500 CP Time (sec.)
12	2	12	2	72	10107.0	3.6×10^{-8}	10x4	4
14	2	14	2	84	8165.6	8.2×10^{-8}	12x4	5
13	3	13	3	117	9498.3	1.8×10^{-7}	22x4	13
12	4	12	4	144	10107.0	6.5×10^{-9}	19x4	19
24	2	24	2	144	5581.3	3.4×10^{-8}	33x4	25
26	2	26	2	156	5576.0	1.6×10^{-7}	50x4	36
28	2	28	2	168	5575.0	6.3×10^{-7}	51x4	43
30	2	30	2	180	5574.6	3.4×10^{-7}	58x4	54
24	4	24	4	288	5581.3	9.9×10^{-7}	79x4	288
10	10	10	10	300	11319.0	5.3×10^{-11}	38x4	142
10	11	10	11	330	10916.0	1.0×10^{-7}	30x4	-
11	10	11	10	330	9910.3	4.2×10^{-8}	27x4	156
28	8	14	4	336	4320.3	4.7×10^{-7}	115x5	922
9	13	9	13	351	11798.0	6.5×10^{-7}	52x4	239
25	5	25	5	375	4070.3	2.0×10^{-8}	43x4	234
26	6	26	6	468	4070.3	4.5×10^{-8}	59x4	536
28	6	28	6	504	4070.0	9.9×10^{-7}	84x4	632
26	7	26	7	546	4071.6	3.7×10^{-5}	40x4	582
27	7	27	7	567	4070.3	7.9×10^{-7}	114x4	964
26	8	26	8	624	4070.6	2.0×10^{-5}	35x4	901

Symmetric circumferential mode

12	2	12	2	71	17295.0	4.8×10^{-7}	19x4	5
14	2	14	2	83	17295.0	6.5×10^{-7}	17x4	6
13	3	13	3	116	16808.0	2.3×10^{-7}	25x4	14
12	4	12	4	143	11073.0	2.2×10^{-7}	8x4	15
24	4	24	4	287	5582.3	4.2×10^{-9}	33x4	114
25	5	25	5	373	4070.3	3.9×10^{-9}	39x4	271
10	17	10	17	539	8383.0	1.9×10^{-7}	27x4	457

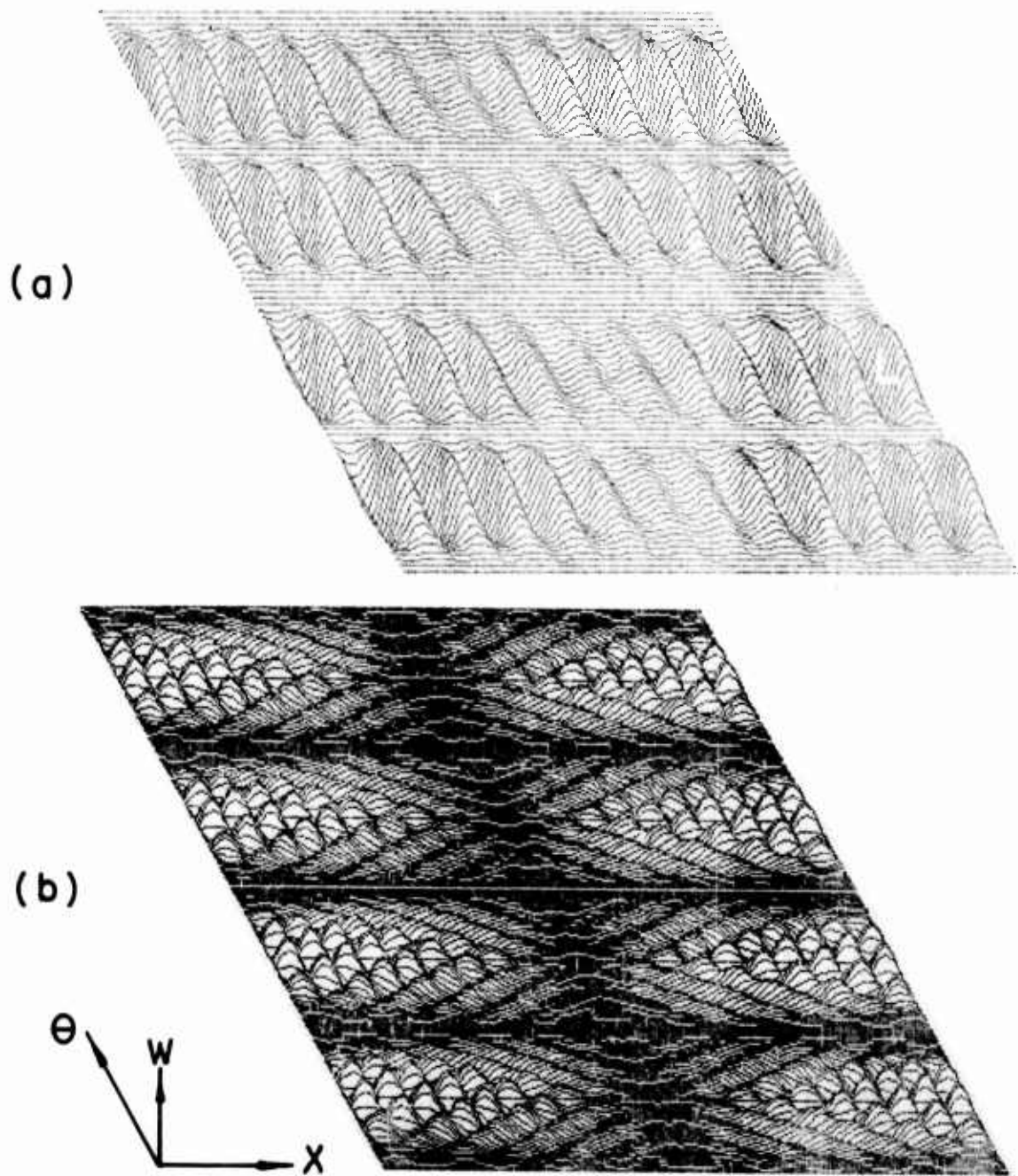


Figure 3 Buckling Mode Shapes for Antisymmetric Circumferential Mode and
 (a) Mixed Longitudinal Modes ($\sigma_x = 4070$ psi; $k_m = 28$; $k_n = 6$;
 $n = 1, 2, \dots, 6$);
 (b) Symmetric Longitudinal Mode ($\sigma_x = 4068$ psi; $k_m = 15$; $k_n = 7$;
 $n = 4, 8, \dots, 28$).

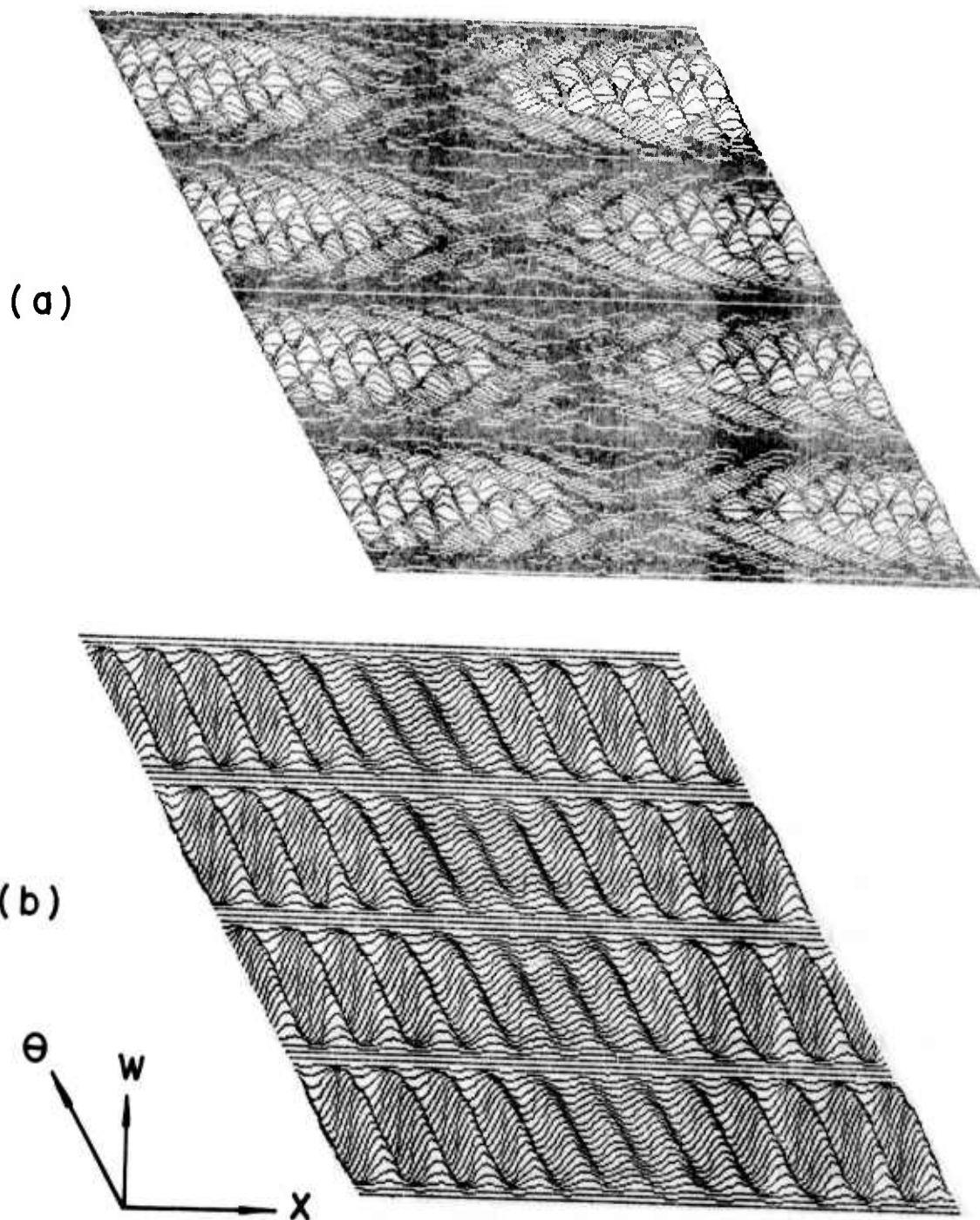


Figure 4 Buckling Mode Shapes for Antisymmetric Longitudinal Mode and
 (a) Symmetric Circumferential Mode ($\sigma_x = 4068.4$ psi; $k_m = 15$;
 $k_n = 7$; $n = 2, 6, \dots, 26$);
 (b) Antisymmetric Circumferential Mode ($\sigma_x = 4068.1$ psi; $k_m = 14$;
 $k_n = 6$; $n = 2, 6, \dots, 22$).

different from one another but the buckling stresses are almost identical ($\sigma_x = 4068$ psi). This buckling stress is very close to that for the same cylinder without stiffeners ($\sigma_x = 4047$ psi; $P_x = 36613$ pounds; $m = 2$; $n = 3$). The results indicate that small number of discrete stiffeners is not effective in raising the buckling strength ($\sigma_x = 4047$ psi) for the same monocoque cylinder even if the mode shapes are drastically changed. In the case of flat plate, however, discrete stiffening increases the buckling strength substantially.

The buckling load for this problem was also calculated based on the uniform strain assumption. The antisymmetric circumferential mode, the antisymmetric longitudinal modes ($m = 2, 4, \dots, 32$), and the circumferentially related modes ($n = 2, 6, \dots, 30$) governed the buckling equations. The buckling values obtained were: $P_x = 21632$ pounds; $\sigma_x = 1639$ psi; $\sigma_\theta = 229.5$ psi. The mode shape is shown in Fig. 5. It is of interest to note that this buckling load is even less than that (36613 pounds) for the same cylinder without stiffeners. This difference is caused by the basic assumptions. In the case of uniform stress assumption, there is no circumferential stress. But in the case of uniform strain assumption, the ring introduces high compressive circumferential stress in the skin that destabilizes the shell.

It is noted that the computing time and storage were drastically reduced in treating the submatrices of smaller sizes in Eqs. (28 and 29).

3. COMPARISON WITH EXPERIMENTAL RESULTS

Esslinger and Geier (Reference 19) tested a series of discretely stiffened Mylar cylinders with edges cast into rigid end plates. The modulus of elasticity of Mylar, which is not available in Reference 19, has a wide range. However, based on the geometric parameter Z of 5320, the Poisson's ratio of 1/3, and the theoretical buckling load of 78 kg given in Reference 19 for a monocoque cylinder, the modulus of elasticity was obtained as 553.6 kg/mm^2 by using the

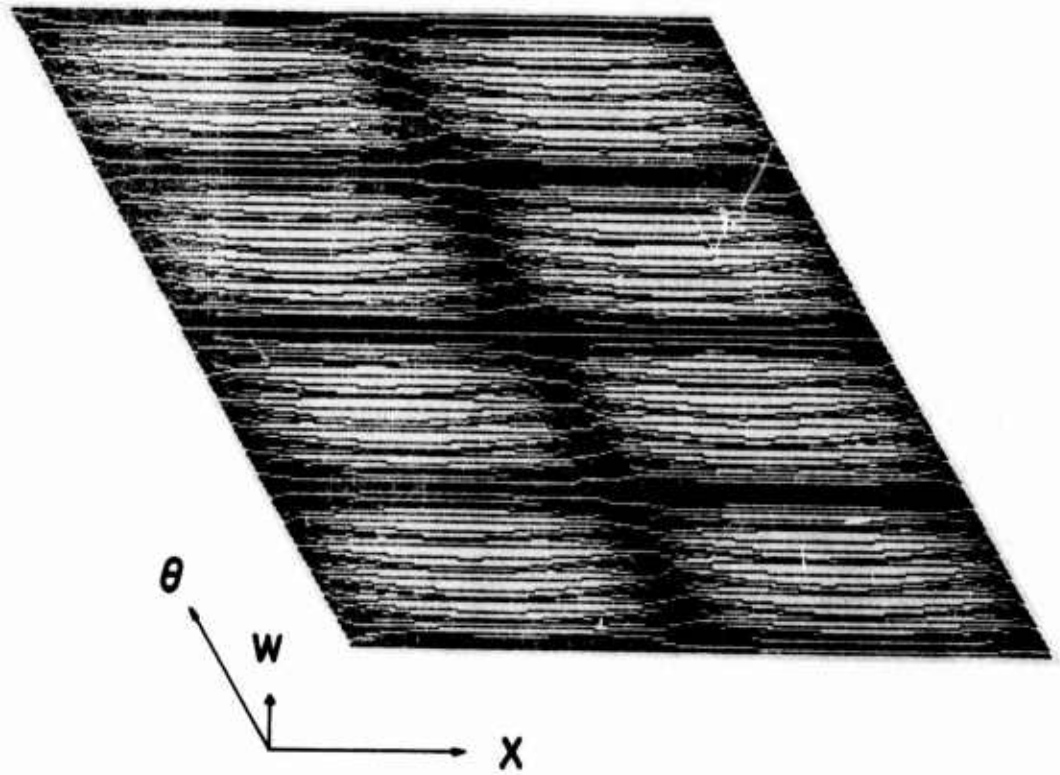


Figure 5 Buckling Mode Shape for Simply-Supported Cylinder With One Ring and Four Stringers under Axial Compression (Uniform Strain Assumption).

classical formula that the Euler buckling stress is $Eh/[3(1-\nu^2)]^{1/2}r$. Two very stiff rings were placed at the ends of the cylinder to simulate the built-in edge conditions that $w = v = \partial w/\partial x = N_x = 0$.

(a) Cylinder With Eight Outer Stringers and Two Inner Rings Under External Pressure

The sizes of the cylinder was defined as: $L = 330\text{mm}$; $r = 100\text{mm}$; $h = 0.193\text{ mm}$. The stiffeners were T-type with two back-to-back angle bars of $6 \times 6 \times 0.193\text{ mm}$.

The buckling computations were based on the antisymmetric circumferential mode, the symmetric longitudinal modes ($m = 1, 3, \dots, 41$), and the circumferentially related modes ($n = 4, 12, 20, \dots, 52$). For the uniform strain and uniform stress assumptions, the buckling pressures obtained were 0.009768 and 0.01002 kg/cm^2 , respectively. Both are in close agreement with the experimental value of 0.0095 kg/cm^2 . The buckling mode shape was plotted in Fig. 6 with $m = 3$ and $n = 12$. The mode shape and mode numbers agree well with those shown in Fig. 11 of Reference 19. For the same cylinder without stiffeners the buckling pressure is only about 0.0039 kg/cm^2 (Reference 19).

(b) Cylinder With Eight Outer Stringers and Two Inner Rings Under Uniform Axial Compression

The cylindrical shell considered was the same as the previous one but all the stiffeners were single angle bars of $6 \times 6 \times 0.193\text{ mm}$.

The stiffeners were first neglected. In the buckling computation, the antisymmetric circumferential mode with $n = 6$ and the symmetric longitudinal modes with $m = 1, 3 \dots, 79$ were used. The buckling load obtained was 78.2 kg which agreed well with the theoretical value of 78 kg given in Reference 19. The buckling mode shape found (with one half longitudinal sine wave) also agreed with the experimental photograph (Reference 19).

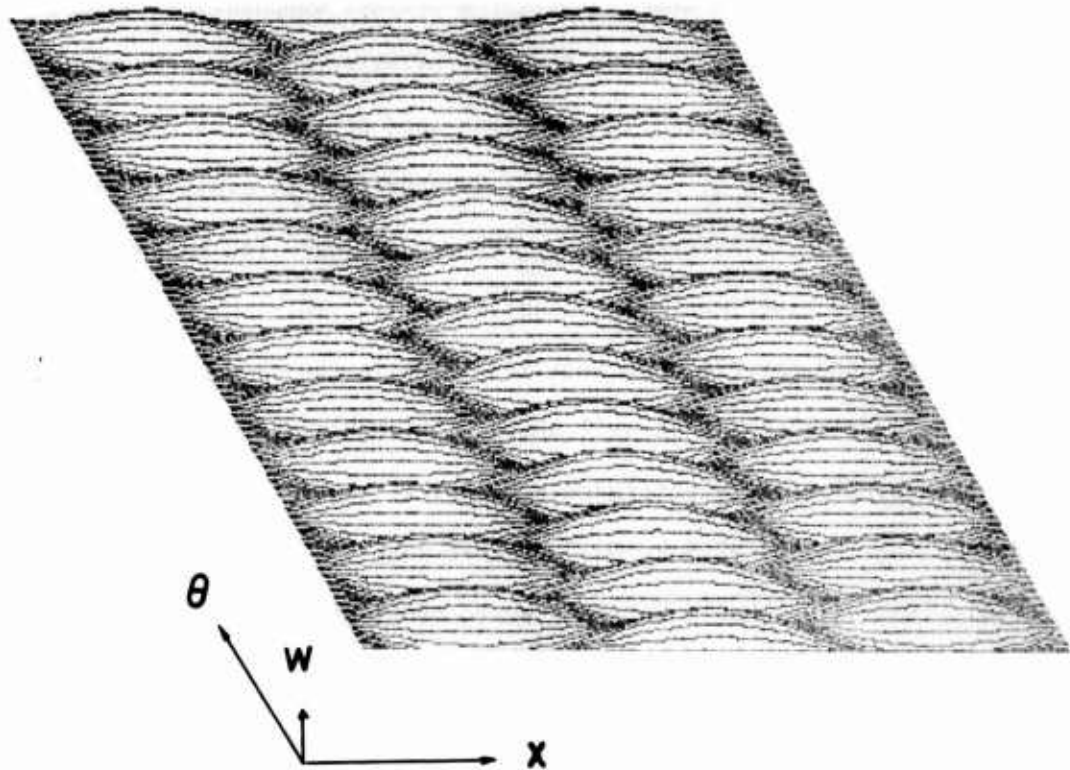


Figure 6 Buckling Mode Shape for Clamped Cylinder With Two Inner Rings and Eight Outer Stringers Under External Pressure.

As to the buckling load of the stiffened shell, Reference 19 provided an experimental value of 45 kg, a theoretical value of 80 kg, and an experimental postbuckling value greater than 95 kg. The present computations were based on the same modes as those used in the case of external pressure. Based on the uniform strain assumption, the buckling load obtained was 75.7 kg. The mode shape is shown in Fig. 7. The 75.7 kg predicted is close to the theoretical value of 80 kg given in Reference 19. The present buckling mode shape agrees well with that obtained experimentally in Reference 19. The lack of agreement between the theoretical and experimental buckling loads in the case of axially compressed monocoque cylindrical shell is well-known. This phenomenon also appears in the present case of discretely stiffened cylindrical shell.

A buckling load of 92.0 kg was obtained when the uniform stress assumption was used. This value should be expected to be higher than that (75.7 kg) obtained by using the uniform strain assumption. The reason lies mainly in the difference in circumferential stress. The circumferential stress is zero in the case of uniform stress, while in the case of uniform strain, it is 2.2% of the longitudinal stress which corresponds to 90.8% of the circumferential buckling stress for the same cylinder without stiffeners under external pressure.

This circumferential stress in the shell is introduced by the two rings in circumferential tension.

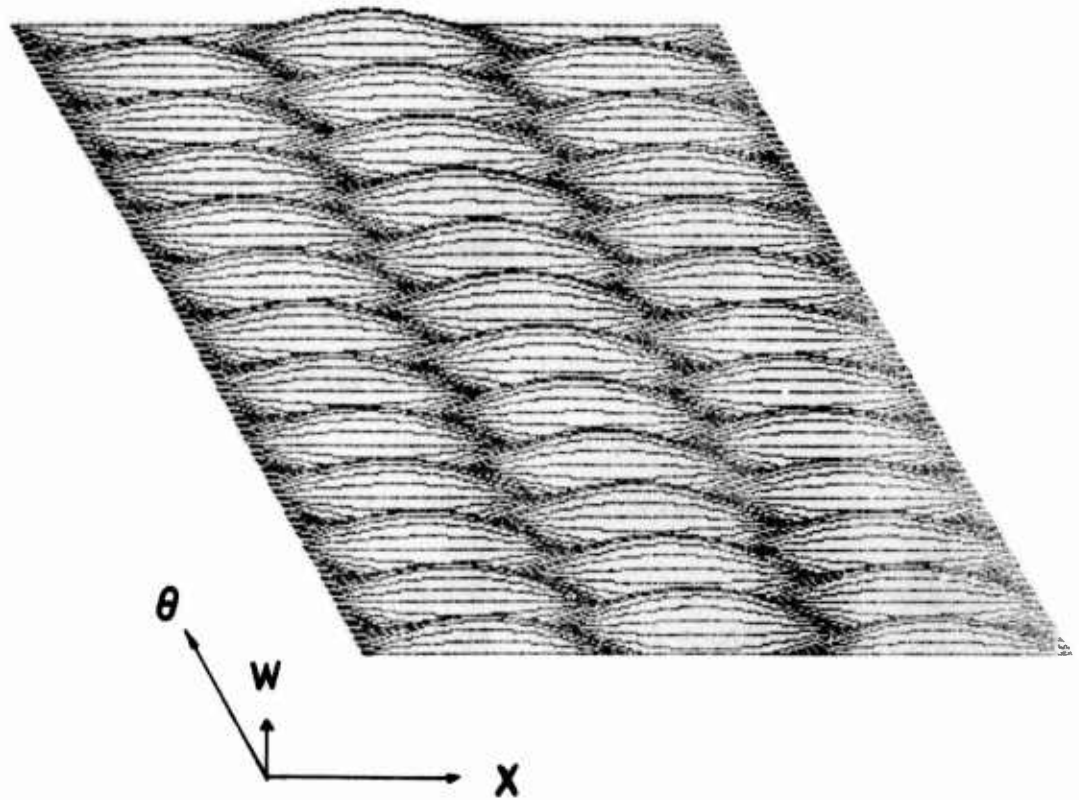


Figure 7 Buckling Mode Shape for Clamped Cylinder With Two Inner Rings and Eight Outer Stringers Under Axial Compression.

SECTION V

WEIGHT, CONSTRAINTS, AND DESIGN VARIABLES

The weight W of an orthogonally stiffened shell with multiple stiffener sizes is expressed as

Weight = weight of the skin + weight of the smeared-out stringers
 + weight of the smeared-out rings - weight of the material
 at the intersections of the smeared-out stringers and
 rings + weight of the discrete stringers + weight of the
 discrete rings - weight of the material at the
 intersections of the discrete stringers and rings

or

$$\begin{aligned}
 W = & 2\pi r L h \rho + 2\pi r L h_{e1} \rho + \pi [2r - \text{sgn}(d_2)(d_2+h)] h_{e2} L \rho \\
 & - \min(|d_1|, |d_2|) \{1 + \text{sgn}(d_1 \cdot d_2)\} / 2 \cdot h_{e1} h_{e2} / |d_1 \cdot d_2| + L \rho \sum_{k=1}^{n_s} A_{S_k} \\
 & + \pi [2r - \text{sgn}(d_r)(d_r+h)] \rho \sum_{k=1}^{n_r} A_{r_k} - \min(|d_s|, |d_r|) \\
 & \{1 + \text{sgn}(d_s \cdot d_r)\} / 2 t_s t_r n_s n_r \rho
 \end{aligned} \tag{1}$$

with

$$\begin{aligned}
 h_{e1} &= d_1 t_1 / a_1 \\
 h_{e2} &= d_2 t_2 (1/a_2 - 1/L) \\
 \text{sgn}(x) &= x/|x|
 \end{aligned} \tag{2}$$

where r , h , L are the mean radius, thickness, and length of the cylindrical shell, respectively; ρ is the material density; d and t are the depth and width of the stiffeners, respectively; the subscripts 1, 2, s, and r are associated with the smeared-out stringer, the smeared-out ring, the discrete stringer, and the discrete ring, respectively; a is the spacing between the

stiffeners; A and n are the cross-sectional area and the total number of the stiffeners (See Figure 1).

For the cylindrical shell with orthogonal smeared-out stiffeners the inequality constraints are defined as follows:

- (1) buckling of the stiffened cylinder

$$\psi_1 = 1 - P_x/P_{x0} \geq 0 \quad (42)$$

where P_{x0} is the general buckling load;

- (2) buckling of the stiffened cylinder between the circumferential rings with two circular edges considered as simply-supported

$$\psi_2 = 1 - P_{xp}/P_{x0} \geq 0; \quad (43)$$

- (3) buckling of the shell skin bounded by longitudinal and circumferential stiffeners with four edges considered as simply-supported

$$\psi_3 = \frac{\pi^2 h^2 E}{3(1-\nu^2) a_1^2} \div \sigma_x - 1 \geq 0; \quad (44)$$

- (4) skin failure by yielding

$$\psi_4 = 1 - (\sigma_x^2 - \sigma_x \sigma_\theta + \sigma_\theta^2) / \sigma_y^2 \geq 0 \quad (45)$$

where σ_y is the yielding stress of the skin;

- (5) longitudinal stringer failure by yielding

$$\psi_5 = 1 - \sigma_{x1} / \sigma_y \geq 0; \quad (46)$$

- (6) circumferential ring failure by yielding

$$\psi_6 = 1 - |\sigma_{\theta 2}| / \sigma_y \geq 0; \quad (47)$$

- (7) buckling of the longitudinal stringer between the circumferential rings with one end free and the other end simply-supported (Reference 44)

$$\psi_7 = \frac{\pi^2 E}{12(1-\nu^2)} \left(\frac{t_1}{d_1}\right)^2 \left[\left(\frac{d_1}{a_2}\right)^2 + 0.425\right] \div \sigma_{x1} - 1 \geq 0; \quad (48)$$

where it is assumed in Eq. (48) that both stringers and rings are on the same side of the skin and that the rings are deeper than the stringers. If these conditions are violated, the spacing a_2 in Eq. (48) should be replaced by the spacing between two discrete rings $L/(1 + n_r)$ on the same side of the skin. In the absence of discrete rings, n_r is zero;

(8) design variable constraints

$$u_{\ell_i} \leq u_i \leq u_{u_i} \quad i = 1, 2, \dots, p \quad (49)$$

or

$$\psi = (u_i - u_{\ell_i})(u_{u_i} - u_i) \geq 0 \quad (50)$$

where the design variables consist of a_1 , a_2 , t_1 , t_2 , d_1 , d_2 , and h .

The design of the cylindrical shell with orthogonal smeared-out stiffeners thus includes seven design variables and fourteen inequality constraints.

For the cylindrical shell with orthogonal smeared-out and discrete stiffeners, the inequality constraints described for the smeared-out case still hold but the computation of the allowable uniform axial buckling load P_{x0} used in Eqs. (3) and (4) should incorporate the effect of discrete stiffeners as well. Besides, three more constraints are included:

(1) longitudinal discrete stringer failure by yielding

$$\psi = 1 - \sigma_{xs}/\sigma_{ys} \geq 0 \quad (51)$$

(2) circumferential discrete ring failure by yielding

$$\psi = 1 - |\sigma_{\theta r}|/\sigma_{yr} \geq 0 \quad (52)$$

- (3) buckling of the longitudinal discrete stringer between two circumferential rings with one end free and the other end simply supported

$$\psi = \frac{\pi^2 E_s}{12(1-\nu_s^2)} \left(\frac{t_s}{d_s}\right)^2 \left[\left(\frac{d_s(1+n_r)}{L}\right)^2 + 0.425\right] \div \sigma_{xs} - 1 \geq 0 \quad (53)$$

It is assumed in Eq. (53) that both stringers and rings are on the same side of the skin and that the rings are deeper than the stringers. If these conditions are violated, n_r should be set equal to zero.

The design variables chosen for this case are a_1 , a_2 , t_1 , t_2 , d_1 , d_2 , h , t_s , d_s , t_r and d_r . The design of the cylindrical shell with both smeared-out and discrete stiffeners thus includes 11 design variables and 21 inequality constraints.

SECTION VI

A SIMPLIFIED BUCKLING FORMULATION

It has been shown in the example 2 of Section IV that for the buckling analysis of a simply supported cylindrical shell with one ring and four stringers under uniform axial compression, the exact formulation required a minimum of 750 eigenvalue equations (with $k'_m = k_m = 25$ and $k'_n = k_n = 5$). With the use of a matrix uncoupling technique based on the associated mode shapes, a matrix reduction technique by partitioning and substitution, a special compact storage scheme to make use of the sparseness of the submatrices, and the Ritz iteration method combined with the Chebyshev eigenvalue solution procedure, the lowest eigenvalue for the 750 equations was able to be solved eventually by a CDC 6500 computer with only approximately 400 seconds of central processing time. Although it has already been a tremendous reduction in computation, 400 seconds are still formidably long if the buckling load has to be computed repeatedly for optimization.

To circumvent this difficulty, the computing time for buckling load must be further reduced drastically and it appears that one has no alternative but to seek for an extremely simple and short method for only rough estimate of buckling load. In that case the exact buckling computation still has, of course, to be performed for the optimized design variables to check the validity of the buckling load obtained by the approximate method.

In the case of cylinder with smeared-out stiffeners, it was shown in Reference 10 that an exact solution can be achieved by using one term for each u , v , and w functions. Thus for extreme simplicity, one anti-symmetric circumferential mode and one longitudinal mode are assumed in the displacement functions for the cylinder with discrete stiffeners.

$$\begin{cases} u = U_{mn} \cos \frac{m\pi x}{L} \sin n\theta \\ v = V_{mn} \sin \frac{m\pi x}{L} \cos n\theta \\ w = W_{mn} \sin \frac{m\pi x}{L} \sin n\theta \end{cases} \quad (54)$$

The displacement functions are substituted into the potential energy expressions (Eq. (1)) and the same procedure as shown in Section II is followed for deriving the buckling equations. The resulting equations are similar to the ones for the cylinder with smeared-out stiffeners and its explicit formulations can be obtained by setting $m=m_i=m_j$ and $n=n_i=n_j$ in Eq.(27) . The critical buckling load is obtained by searching for the smallest eigenvalue in a set of three equations by varying the values of integers m and n .

In the case of cylinders with smeared-out stiffeners a smooth surface for the minimum eigenvalue is obtained so that the efficient sectioning approach proposed and demonstrated in Reference 37 may be used for the search for the minimum. In the case of cylinders with discrete stiffeners, there are many local minima in the eigenvalue surface. The absolute minimum has to be searched for by varying m and n continuously in a certain range. In spite of this disadvantage, this simple approximate discrete calculation is superior to the smeared-out calculation in the buckling prediction of cylinder with discrete stiffeners.

This approximate discrete method was first verified by performing a buckling computation of a cylinder with 100 stringers and 16 rings. The material and geometry parameters of the cylinder are defined as: $E = 1.06 \times 10^7$ psi; $\nu = 1/3$; $a_1 = a_2 = 3$ in.; $d_1 = d_2 = 0.2$ in.; $t_1 = t_2 = 0.125$ in.; $h = 0.05$ in.; $r = 48$ in.; and $L = 50$ in. The exact solution obtained by the exact discrete formulation was given in Section IV. The buckling load was 801.3 lbs/in and the buckling mode numbers were $m = 6$ and $n = 17$. The present approximate discrete computation gave a buckling load of 807.9 lbs/in with the mode numbers $m = 6$ and $n = 17$. It is noted that in order to obtain the converged solutions by using the discrete formulations, 600 degrees of freedom were required while in this approximate method only three degrees of freedom were used.

This approximate discrete method was then tested for a cylinder with only one ring and four stringers. The material and geometry parameters of the cylinder are defined as: $E = 10.6 \times 10^6$ psi; $\nu = 1/3$; $h = 0.03$ in.; $r = 48$ in.; $L = 50$ in.; $d_s = d_r = 1.3196$ in.; $t_s = t_r = 0.8248$ in. The exact converged buckling stress was given in Section IV as 4068 psi with several different mode shapes. The present discrete approximate method gave a buckling stress of 5008 psi with buckling mode numbers $m = 24$ and $n = 2$.

It is important to note that when the seven sets of near minimum eigenvalue solutions for the above examples were obtained in Section IV, the sizes of the originally coupled eigenvalue equations were: 504; 630; 750; 936; 1008; 1134; and 1248. If the present approximate method is used, only three eigenvalue equations need be solved. The loss in accuracy is compensated for by the drastic reduction in computing time. Without such drastic reduction the optimization computations will be too expensive to perform. The buckling load for the optimized design

variables obtained by this approximate method is, however, checked by the expensive exact discrete computation. The difference in the predicted buckling loads between this approximate discrete method and the exact discrete method becomes smaller as the number of stiffeners is increased. As will be shown in a subsequent example of minimum weight design, the buckling load predicted by this approximate method for a cylinder with 5 discrete rings and 30 discrete stringers is very close to the exact discrete solution.

SECTION VII
THEORY OF OPTIMIZATION

The theory of optimization has long been an attractive research topic and extensive research works have been done. Various theories of optimization have been applied to the minimum weight design of structures with various constraints. These applications have been discussed in the Introduction.

In Reference 40, Schuldt developed a method of multipliers for mathematical programming problems with equality and inequality constraints. Since this method has not been applied to the minimum weight design of structures, it is introduced here as an efficient method for the minimum weight design of the stiffened cylindrical shell with multiple stiffener sizes.

The conventional problem of optimum design is to minimize the weight of a structure expressed as a function of the design variables which satisfy a series of constraints on the design behavior and on the sizes of the variables (design variable equality constraints or design variable inequality constraints). That is, to minimize

$$W(\tilde{u}) \tag{55}$$

$$\text{subject to } \tilde{\phi}(\tilde{u}) = \tilde{0}$$

$$\tilde{\psi}(\tilde{u}) \geq \tilde{0} \tag{56}$$

According to Reference 40 the problem may be transformed into the one of minimizing the augmented function

$$F(\tilde{u}, \tilde{\lambda}, \tilde{\mu}) = W(\tilde{u}) + \tilde{\lambda}^T \tilde{\phi}(\tilde{u}) - \tilde{\mu}^T \tilde{\psi}(\tilde{u}) \tag{57}$$

subject to

$$\tilde{\phi}(\tilde{u}) = \tilde{0} \quad (58)$$

$$\tilde{\psi}(\tilde{u}) \geq \tilde{0} \quad (59)$$

which satisfy the following first-order condition at the solution point.

$$F_u(\tilde{u}, \tilde{\lambda}, \tilde{\mu}) = W_u(\tilde{u}) + \tilde{\phi}_u(\tilde{u})\tilde{\lambda} - \tilde{\psi}_u(\tilde{u})\tilde{\mu} = 0 \quad (60)$$

$$\mu_{(j)} \psi_{(j)}(\tilde{u}) = 0 \quad j=1, \dots, r \quad (61)$$

$$\mu_{(j)} \geq 0 \quad j=1, \dots, r \quad (62)$$

The augmented penalty function is written as

$$\Omega(\tilde{u}, \tilde{\lambda}, \tilde{\mu}, k) = Q(\tilde{u}, \tilde{\lambda}, k) + R(\tilde{u}, \tilde{\mu}, k) \quad (63)$$

where

$$\begin{aligned} Q &= W(\tilde{u}) + \tilde{\lambda}^T \tilde{\phi}(\tilde{u}) + k \tilde{\phi}^T(\tilde{u}) \tilde{\phi}(\tilde{u}) \\ &= W(\tilde{u}) + k [\tilde{\phi}(\tilde{u}) + \frac{1}{2k} \tilde{\lambda}]^T [\tilde{\phi}(\tilde{u}) + \frac{1}{2k} \tilde{\lambda}] - \frac{1}{4k} \tilde{\lambda}^T \tilde{\lambda} \end{aligned} \quad (64)$$

$$R = k [\tilde{\psi}(\tilde{u}) - \frac{1}{2k} \tilde{\mu}]^T [\tilde{\psi}(\tilde{u}) - \frac{1}{2k} \tilde{\mu}] - \frac{1}{4k} \tilde{\mu}^T \tilde{\mu} \quad (65)$$

$$\psi_j(\tilde{u}) = \min[\psi_{(j)}(\tilde{u}), \frac{1}{2k} \mu_{(j)}] \quad j=1, \dots, r \quad (66)$$

The constant k is initially chosen from scaling consideration and held fixed throughout the algorithm.

Initial cycle is begun with the choice of $\tilde{\lambda} = \tilde{0}$ and $\tilde{\mu} = \tilde{0}$, i.e.,

$$\Omega(\tilde{u}, \tilde{0}, \tilde{0}, k) = W(\tilde{u}) + k [\tilde{\phi}^T(\tilde{u}) \tilde{\phi}(\tilde{u}) + \tilde{\psi}^T(\tilde{u}) \tilde{\psi}(\tilde{u})] \quad (67)$$

where

$$\tilde{\psi}_j(x) = \min\{\psi_j(x), 0\} \quad j=1, \dots, r \quad (68)$$

The following multiplier updating rules are applied,

$$\tilde{\lambda}_2 = \tilde{\lambda}_1 + 2k \tilde{\phi}(x) \quad (69)$$

$$\tilde{\mu}_2 = \tilde{\mu}_1 - 2k \tilde{\psi}(x) \quad (70)$$

where subscripts 1 and 2 correspond to the current and the next cycles, respectively.

Differentiating Eq. (63) with respect to the design variables \tilde{u} , the following necessary conditions for the minimum is obtained,

$$\Omega_u(\tilde{u}, \tilde{\lambda}, \tilde{\mu}, k) = W_u(\tilde{u}) + \tilde{\phi}_u(\tilde{u})[\tilde{\lambda} + 2k \tilde{\phi}(\tilde{u})] - \tilde{\psi}(\tilde{u})[\tilde{\mu} - 2k \tilde{\psi}(\tilde{u})] = 0 \quad (71)$$

Combining Eqs. (69), (70), and (71), one may obtain the following expression where the updated multipliers satisfy the optimality condition given by Eq. (60)

$$F_u(\tilde{u}, \tilde{\lambda}_2, \tilde{\mu}_2) = W_u(\tilde{u}) + \tilde{\phi}_u(\tilde{u})\tilde{\lambda}_2 - \tilde{\psi}_u(\tilde{u})\tilde{\mu}_2 = 0 \quad (72)$$

In addition to this condition, the equality constraints by Eq. (58) and the inequality constraints defined by Eq. (59) should be satisfied. In Reference 40 Schuldt first showed that the augmented penalty function increases at the end of each minimization cycle when the multipliers are changed from $\tilde{\lambda}_1$ and $\tilde{\mu}_1$ to $\tilde{\lambda}_2$ and $\tilde{\mu}_2$, respectively. He then demonstrated through one example that succeeding cycles of minimizing the augmented penalty function may drive toward constrained satisfaction.

In order to minimize the augmented penalty function Ω defined by Eq. (63), the method for the unconstrained function minimization pro-

posed by Fletcher and Powell (Reference 45) and a quasi-Newton method are used. The two methods are also compared.

All gradient calculations are carried out by the simple finite difference method in this study.

SECTION VIII

TWO OPTIMUM WEIGHT DESIGN EXAMPLES

The first design example chosen was a simply-supported orthogonally stiffened cylindrical shell subjected to uniform axial compression. The cylinder had a radius of 48 inches and a length of 50 inches. The properties of the aluminum were used for both the cylinder and the stiffeners: $E = 10.6 \times 10^6$ psi; $\nu = 1/3$; $\rho = 0.101$ lbs/in³. The buckling load of $P_{x0} = 238.2$ kips or $N_{x0} = 789.8$ lbs/in was used as the buckling constraint. The seven initial design variables which were restrained between 0.01 and 10 inches are shown in Table 4. This problem is similar to the one given in Reference 37 but with one extra design variable a_2 .

The buckling computation was based on the simple smeared-out formulation and the optimization process was performed by the method of multipliers with the Fletcher-Powell method as well as the quasi-Newton method. One of the purposes of choosing this example was to obtain data for comparison with a later example with additional discrete stiffeners. The other purpose of conducting this example was to evaluate the performance of the present optimization methods. The results for the minimum weight design are presented in Table 4. For this example the Fletcher-Powell method seems to be more suitable than the quasi-Newton method.

The second example was a simply-supported aluminum cylindrical shell with 5 discrete rings, 30 discrete stringers, and smeared-out stiffeners. The cylinder had the same length, radius, and material properties as the first example. The buckling constraint was 789.82 lbs/in. The 11 initial design variables which were restrained between 0.01 and 10 inches are shown in Table 5.

Table 4 Weight minimization using the smeared-out formulation

($N_{x0} = 789.82$ lbs/in.; $\sigma_y = 50$ ksi; 0.01 in. $\leq u_i \leq 10$ in.,
 $i=1,2,\dots,7$)

Iteration Number	Number of Function Evaluations	Weight (lbs.)	Buckling Stress N_x (lbs/in) ^x	Mode Number		a_1 (in)	a_2 (in)
				m	n		
0	0	124.63	913.5	4	15	1.0	3.0
20	2334	45.23	789.5	6	7	0.5645	4.962
0	0	124.63	913.5	4	15	1.0	3.0
11	915	51.22	788.0	4	11	0.8125	4.454

d_1 (in)	d_2 (in)	t_1 (in)	t_2 (in)	h (in)	CDC 6500 CP time (sec)	Method
0.2 0.2737	0.2 1.7077	0.125 0.02287	0.125 0.00999	0.05 0.01559	0 2315	Fletcher-Powell
0.2 0.3318	0.2 0.8337	0.125 0.02546	0.125 0.01181	0.05 0.02126	0 879	quasi-Newton

Table 5 Weight minimization using smeared-out and discrete formulations

($N_{x0} = 789.82$ lbs/in.; $\sigma_y = 50$ ksi; 0.01 in. $\leq u_i \leq 10$ in. with $i=1,2,\dots,11$; $n_s = 30$; $n_r = 5$)

Iteration Number	NFE*	Weight (lbs.)	N_x (lbs/in)	Mode		a_1 (in.)	a_2 (in.)	d_1 (in.)	d_2 (in.)
				m	n				
0	0	141.21	1102.8	3	14	1.0000	3.0000	0.2000	0.2000
15	1636	42.83	815.8	11	15	0.3321	2.7754	0.1715	1.0446
0	0	141.21	1102.8	3	14	1.0000	3.0000	0.2000	0.2000
11	934	78.01	792.1	7	15	1.0109	3.0003	0.1759	0.2619

t_1 (in.)	t_2 (in.)	h (in.)	d_s (in.)	t_s (in.)	d_r (in.)	t_r (in.)	T^+ (sec.)	Method
0.1250	0.1250	0.0500	0.4085	0.2553	0.0913	0.0571	0	Fletcher-
0.0156	0.0110	0.0100	0.6938	0.0896	0.0145	0.0321	1711	Powell
0.1250	0.1250	0.0500	0.4085	0.2553	0.0913	0.0571	0	quasi-
0.0361	0.1192	0.0230	0.4414	0.2741	0.0892	0.0509	841	Newton

* Number of function evaluations

+ CDC 6500 central processing time

The buckling computation during the weight minimization was performed using the present approximate discrete technique. The results of the minimum weight design are given in Table 5. The approximate buckling load for the minimum weight design obtained by using the Fletcher-Powell method was also checked by using the exact buckling computation based on the discrete formulation. The symmetrical longitudinal modes with $m = 1, 3, 5, \dots, 59$, the antisymmetric circumferential modes, and the circumferentially related modes with $n = 7, 23, 37, 53$ governed the buckling equations. The exact buckling load obtained was 801.7 lbs/in which was very close to the 815.8 lbs/in obtained by the approximate discrete method. The corresponding mode shape is shown in Fig. 8. This optimized mode shape shows that a very smooth buckling surface resulted from the combined effect of the smeared-out stiffeners and the discrete stiffeners.

Again, Table 5 reveals that the Fletcher-Powell method is more suitable in the present weight minimization than the quasi-Newton method.

The process of the weight minimization by using the Fletcher-Powell method is summarized in Table 6. The weight reduction was completed in the early stage of the optimization but the violation of the constraints was sometimes greater than ten percent. The rest of the optimization cycles was carried out to correct the violations. All the final designs violated the constraints by less than one percent.

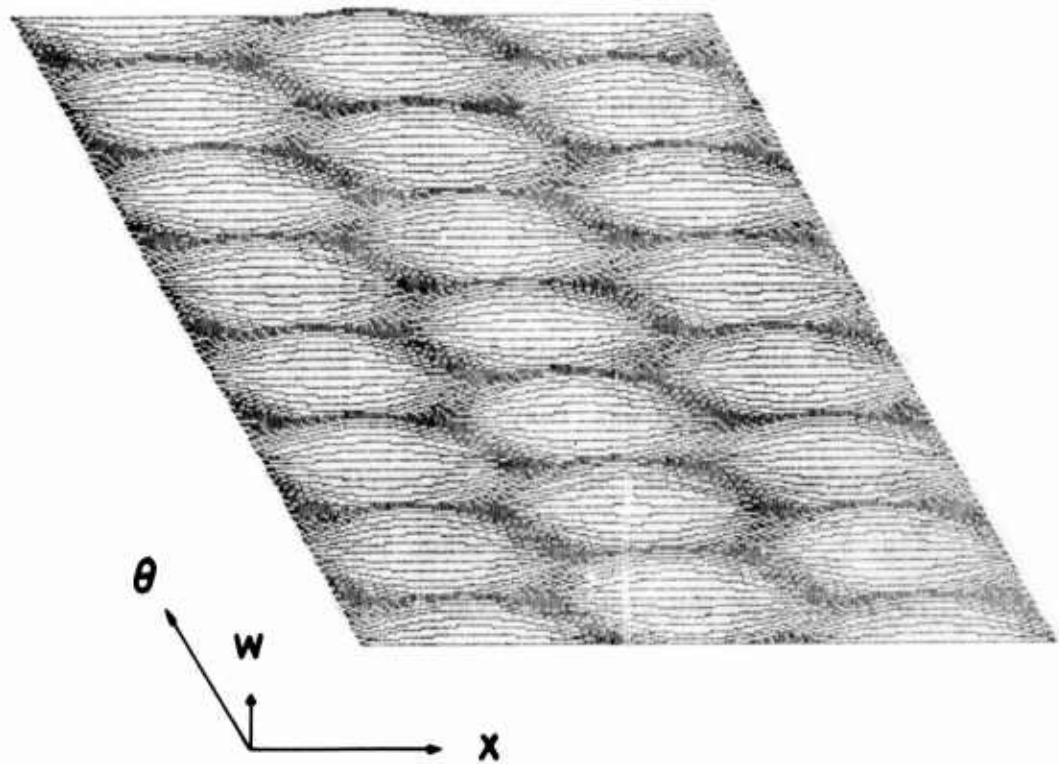


Figure 8 Buckling Mode Shape for the Optimized Cylindrical Shell
With Smeared-out and Discrete Stiffeners.

Table 6 Process of the Weight Minimization by the Fletcher-Powell
Method

Iteration Number	Number of Function Evaluations	CDC 6500 CP Time (Sec.)	Weight (lbs.)	Formulation
0	0	0	124.63	Smeared-out
5	538	594	54.50	
10	1098	1194	49.32	
14	1702	1709	46.38	
20	2334	2315	45.23	
0	0	0	141.21	Smeared-out and discrete
4	408	444	48.10	
9	912	968	45.62	
11	1144	1203	43.85	
15	1636	1711	42.83	

The optimized stiffened shell with single stiffener size has the failure modes of general buckling and buckling of the shell skin bounded by longitudinal and circumferential stiffeners, expressed by Eq. (42) and Eq. (44), respectively. The optimized stiffened shell with multiple stiffener sizes is inside the feasible region and near the failure modes of general buckling, buckling of the shell skin, and buckling of the smeared-out longitudinal stringer, expressed by Eq. (42), Eq. (44) and Eq. (48), respectively.

The present examples show that the method of multipliers with the Fletcher-Powell method is very effective in the weight minimization. The results in Table 6 show that under the same buckling constraint the cylinder with smeared-out and discrete stiffeners results in less weight than the ordinary cylinder with only smeared-out stiffeners.

SECTION IX
CONCLUDING REMARKS

The buckling equations for the cylindrical shell with multiple stiffener sizes are formulated using the energy method. For the case of equally spaced and identical stringers and equally spaced and identical rings, a close examination of the buckling equations leads to the uncoupling of the buckling equations into separate sets of equations associated with the symmetric and antisymmetric longitudinal modes, symmetric and antisymmetric circumferential modes, and circumferentially related modes. By using such uncoupling and some matrix partitioning and reduction, the huge sets of matrix equations required for the buckling predictions of a common discretely stiffened cylinder can be reduced drastically to manageable sizes. Effort is made to preserve the sparseness of the buckling matrices so that a special compact storage technique can be used.

A method, the Ritz iteration with Chebyshev procedure, is developed for efficient computation of the minimum eigenvalue of a large general eigenvalue problem. The superiority of this method over other methods is demonstrated through a numerical example.

The discrete formulations are first used to analyze an axially compressed cylinder with a large number of stiffeners for which an alternative solution based on the smeared-out method can be obtained for comparison. The agreements are very good for the formulations based on both the uniform stress and uniform strain assumptions (see Table 2). The formulations are then verified by comparing the computed buckling loads and modes with the experimental results for a clamped cylinder with two rings and eight

stringers under external pressure and then under axial compression. For the case of external pressure, the agreements are good for the formulations based on both the uniform stress and uniform strain assumptions. For the case of axial compression, the agreements are poor. Such lack of agreement between theoretical and experimental axial buckling loads has long existed in the case of monocoque cylinder.

It should be noted that both the uniform stress and uniform strain assumptions are shown to be consistent with each other and correct for the cylinder under external pressure. This is the important case where a small number of discrete stiffeners is found to be very effective in raising the buckling loads. Such conclusion was made previously by Esslinger and Geier in an experimental study. For the case of axial compression, the two prestress assumptions do not result in the same buckling load. The uniform strain assumption results in circumferential compression in the skin and consequently, results in lower buckling load than the uniform stress assumption. However, this is the unimportant case where a small number of discrete stiffeners is found to be ineffective in raising the buckling loads.

The minimum weight design of orthogonally stiffened cylindrical shells with discrete stiffeners in addition to the smeared-out stiffeners has not been studied before mainly due to the computational difficulty in obtaining the buckling load. With the development in Sections II, III, and IV, which formulated the discrete stiffeners exactly and simplified the computational method tremendously, such computational difficulty was reduced. The simplifications included uncoupling the buckling matrix based on the associated mode shapes, reducing the uncoupled submatrices by partitioning and substitution, taking advantage of the sparseness of the

buckling matrix by a special compact storage scheme, and using an efficient eigenvalue solution procedure. The development is, however, still too expensive to be used repeatedly for weight minimization.

In this report, an approximate discrete formulation based on very simple displacement functions has been suggested for computing the buckling load for the discretely stiffened cylinders. This method requires the solution of a set of only three instead of several hundred eigenvalue equations. The difficulty in computing time for the weight minimization has thus been overcome. To ensure that the optimized design using this approximate discrete method for predicting buckling loads is valid, the exact discrete buckling computation is still performed based on the final design variables.

To cope with this simple discrete method for buckling computation, the methods of multipliers with the Fletcher-Powell method and with quasi-Newton method have been chosen for the weight optimization. Two design examples have been performed.

The design examples have provided the following indications:

(1) The present simple discrete method is very effective in weight minimization design. The second example shows that the buckling load predicted by this approximate method was very close to the exact solution.

(2) The comparison shows that for unconstrained minimization the Fletcher-Powell method is more suitable than the quasi-Newton method. The former method is very effective in dealing with the present type of weight minimization problem.

(3) For the minimum weight design of cylindrical shell under buckling constraints, the cylinder with both the smeared-out and the discrete stiffeners can be lighter than the cylinder with only smeared-out stiffeners.

Finally, it should be noted that the above indications are obtained from only two design examples and they should not be regarded as general conclusions.

REFERENCES

1. Van der Neut, A., "The General Instability of Stiffened Cylindrical Shells under Axial Compression", National Luchtvaartlaboratorium Rept. 314, 1947.
2. Block, D. L., Card, M. F., and Mikulas, M. M., "Buckling of Eccentrically Stiffened Orthotropic Cylinders", NASA TN D-2960, Aug. 1965.
3. Card, M. F. and Jones, R. M., "Experimental and Theoretical Results for Buckling of Eccentrically Stiffened Cylinders", NASA TN D-3639, Oct. 1966.
4. Stuhlman, C., DeLuzio, A., and Almroth, B., "Influence of Stiffener Eccentricity and End Moment on Stability of Cylinders in Compression", AIAA Journal, Vol. 4, May 1966, pp. 872-877.
5. Simitzes, G. J., "Instability of Orthotropic Cylindrical Shells under Combined Torsion and Hydrostatic Pressure", AIAA Journal, 5, Aug. 1967, pp. 1463-1469.
6. Simitzes, G. J., "A Note on the General Instability of Eccentrically Stiffened Cylinders", Journal of Aircraft, Vol. 4, Sept.-Oct., 1967, pp. 473-475.
7. Singer, J., Baruch, M., and Harari, O., "On the Stability of Eccentrically Stiffened Cylindrical Shells under Axial Compression", International Journal of Solids and Structures, Vol. 3, 1967, pp. 445-470.
8. Jones, R. M., "Buckling of Circular Cylindrical Shells with Multiple Orthotropic Layers and Eccentric Stiffeners", AIAA Journal, Vol. 6, Dec. 1968, pp. 2301-2305.
9. Simitzes, G. J., "Buckling of Eccentrically Stiffened Cylinders under Combined Loads," AIAA Journal, Vol. 7, Feb. 1969, pp. 335-337.
10. Baig, M. I. and Yang, T. Y., "Buckling Analysis of Orthogonally Stiffened Waffle Cylinders", Journal of Spacecraft and Rockets, Vol. 11, Dec. 1974,

pp. 832-837.

11. MacNeal, R. H., Winemiller, A. F., and Bailie, J. A., "Elastic Stability of Cylindrical Shells Reinforced by One or Two Frames and Subjected to External Radial Pressure", AIAA Journal, Vol. 4, Aug. 1966, pp. 1431-1433.
12. Wang, J. T. S. and Lin, Y. J., "Stability of Discretely Stringer-Stiffened Cylindrical Shells", AIAA Journal, Vol. 11, June 1973, pp. 810-814.
13. Singer, J., and Haftka, R. T., "Buckling of Discretely Stringer-Stiffened Cylindrical Shells and Elastically Restrained Panels", AIAA Journal, Vol. 13, July 1975, pp. 849-850.
14. Egle, D. M. and Sewall, J. L., "An Analysis of Free Vibration of Orthogonally Stiffened Cylindrical Shells with Stiffeners treated as Discrete Elements," AIAA Journal, Vol. 6, March 1968, pp. 518-526.
15. McDonald, D., "A Problem in the Free Vibration of Stiffened Cylindrical Shells," AIAA Journal, Vol. 8, Feb. 1970, pp. 252-258.
16. Wang, J. T. S., "Orthogonally Stiffened Cylindrical Shells Subjected to Internal Pressure", AIAA Journal, Vol. 8, March 1970, pp. 455-461.
17. Soong, T. C., "Buckling of Cylindrical Shells with Intermittently Attached Stiffeners", AIAA Journal, Vol. 8, May 1970, pp. 928-936.
18. Rutishauser, H., "Computational Aspects of F. L. Bauer's Simultaneous Iteration Method", Numerical Mathematics, Vol. 13, 1969, pp. 4-13.
19. Esslinger, M. and Geier, B., "Buckling and Postbuckling Behavior of Discretely Stiffened Thin-Walled Circular Cylinders," Z. Flugwiss, Vol. 18, 1970, pp. 246-253.
20. Kunoo, K., "Minimum Weight Design of Cylindrical Shell with Multiple Stiffener Sizes under Buckling Constraints," Ph.D. Thesis, Purdue University, W. Lafayette, Indiana, 1977.

21. Gerard, G., "Optimum Structural Design Concepts for Aerospace Vehicles", Journal of Spacecraft and Rockets, Vol. 3, Jan. 1966, pp. 5-18.
22. Burns, A. B. and Almroth, B. O., "Structural Optimization of Axially Compressed Ring-Stringer Stiffened Cylinders", Journal of Spacecraft and Rockets, Vol. 3, Jan. 1966, pp. 19-25.
23. Burns, A. B. and Skogh, J., "Combined Loads Minimum Weight Analysis of Stiffened Plates and Shells", Journal of Spacecraft and Rockets, Vol. 3, Feb. 1966, pp. 235-240.
24. Kicher, T. P., "Structural Synthesis of Integrally Stiffened Cylinders", Journal of Spacecraft and Rockets, Vol. 5, Jan. 1968, pp. 62-67.
25. Schmit, L. A., Jr., Morrow, W. M., and Kicher, T. P., "A Structural Synthesis Capability for Integrally Stiffened Cylindrical Shells", AIAA Paper 68-327, Palm Springs, Calif, 1968.
26. Morrow, W. M. and Schmit, L. A., Jr., "Structural Synthesis of a Stiffened Cylinder", NASA CR-1217, Dec. 1968.
27. Lakshmikantham, C. and Gerard, G., "Minimum Weight Design of Stiffened Cylinders", Aeronautical Quarterly, Vol. 21, Feb. 1970, pp. 49-68.
28. Pappas, M. and Amba-Rao, C. L., "A Direct Search Algorithm for Automated Optimum Structural Design", AIAA Journal, Vol. 9, March 1971, pp. 387-393.
29. Hyman, B. I. and Lucas, A. W., "An Optimum Design for the Instability of Cylindrical Shells under Lateral Pressure", AIAA Journal, Vol. 9, April 1971, pp. 738-740.
30. Block, D. L., "Minimum Weight Design for Axially Compressed Ring and Stringer Stiffened Cylindrical Shells", NASA CR-1766, July 1971.

31. Jones, R. T. and Hague, D. S., "Application of Multi-Variable Search Technique to Structural Design Optimization", NASA CR-2038, Jan. 1972.
32. Thornton, W. A., "Synthesis of Stiffened Conical Shells", Journal of Spacecraft and Rockets, Vol. 9, March 1972, pp. 189-195.
33. Shideler, J. L., Anderson, M. S., and Jackson, L. R., "Optimum Mass Strength Analysis for Orthotropic Ring Stiffened Cylinders under Axial Compression", NASA TN D-6772, July 1972.
34. Rehfield, L. W., "Design of Stiffened Cylinders to Resist Axial Compression", Journal of Spacecraft and Rockets, Vol. 10, May 1973, pp. 346-349.
35. Simitzes, G. T. and Ungbhakorn, V., "Weight Optimization of Stiffened Cylinders under Axial Compression", Computers and Structures, Vol. 5, 1975, pp. 305-314.
36. Simitzes, G. T. and Aswani, M., "Minimum Weight Design of Stiffened Cylinder under Hydrostatic Pressure", AIAA Paper 75-138, Pasadena, Calif. Jan. 1975.
37. Kunoo, K. and Yang, T. Y., "Minimum Weight Design of an Orthogonally Stiffened Waffle Cylindrical Shell with Buckling Constraints", Journal of Spacecraft and Rockets, Vol. 13, March 1976, pp. 137-143.
38. Hofmeister, L. D. and Felton, L. P., "Waffle Plates with Multiple Rib Sizes: I. Stability Analysis", Journal of Spacecraft and Rockets, Vol. 7, Nov. 1970, pp. 1322-1327.
39. Hofmeister, L. D. and Felton, L. P., "Waffle Plates with Multiple Rib Sizes: II. Design Examples", Journal of Spacecraft and Rockets, Vol. 7, Nov. 1970, pp. 1327-1331.

40. Schuldt, S. B., "A Method of Multipliers for Mathematical Programming Problems with Equality and Inequality Constraints", *Journal of Optimization Theory and Applications*, Vol. 17, 1975, pp. 155-161.
41. Jolley, L. B. W., Summation of Series, Dover, New York, 1961, pp. 78-79.
42. Wang, C. T., Applied Elasticity, McGraw-Hill, New York, 1953, p. 89.
43. Lancaster, P., Theory of Matrices, Academic Press, New York, 1969, pp. 59-73.
44. Bleich, F., Buckling Strength of Metal Structures, McGraw-Hill, New York, 1952, pp. 327-329.
45. Fletcher, R. and Powell, M. J. D., "A Rapid Descent Method for Minimization", *Computer Journal*, Vol. 6, 1963, pp. 163-168.

THIS REPORT HAS BEEN DELIMITED
AND CLEARED FOR PUBLIC RELEASE
UNDER DOD DIRECTIVE 5200.20 AND
NO RESTRICTIONS ARE IMPOSED UPON
ITS USE AND DISCLOSURE.

DISTRIBUTION STATEMENT A

APPROVED FOR PUBLIC RELEASE

DISTRIBUTION UNLIMITED